

Army Research Laboratory



**Anomalies Incurred by E³ Tests Made
in the Near Field**

Joy L. Arthur
Survivability/Lethality Analysis Directorate
Information & Electronic Protection Division

and

Dr. Glenn Brown
REAP

19990310 010

ARL-TR-1733

February 1999

Approved for public release; distribution unlimited.

QUALITY INSPECTED 1

Preceding Page^S Blank

NOTICES

Disclaimers

The findings in this report are not to be construed as an official Department of the Army position unless so designated by other authorized documents.

Citation of manufacturer's or trade names does not constitute an official endorsement or approval of the use thereof.

REPORT DOCUMENTATION PAGE		Form Approved OMB No. 0704-0188	
Public reporting burden for this collection of information is estimated to average 1 hour per response, including the time for reviewing instructions, searching existing data sources, gathering and maintaining the data needed, and completing and reviewing the collection of information. Send comments regarding this burden estimate or any other aspect of this collection of information, including suggestions for reducing the burden to Washington Headquarters Services, Directorate for Information Operations and Reports, 1215 Jefferson Davis Highway, Suite 1204, Arlington, VA 22202-4302 and to the Office of Management and Budget, Paperwork Reduction Project (0704-0188), Washington, DC 20503.			
1. AGENCY USE ONLY (Leave Blank)	2. REPORT DATE February 1999	3. REPORT TYPE AND DATES COVERED Final	
4. TITLE AND SUBTITLE Anomalies Incurred by E ³ Tests Made in the Near Field		5. FUNDING NUMBERS	
6. AUTHOR(S) Joy L. Arthur (SLAD) Dr. Glenn Brown (REAP)			
7. PERFORMING ORGANIZATION NAME(S) AND ADDRESS(ES) U.S. Army Research Laboratory Survivability/Lethality Analysis Directorate Attn: AMSRL-SL-EV White Sands Missile Range, NM 88002-5513		8. PERFORMING ORGANIZATION REPORT NUMBER ARL-TR-1733	
9. SPONSORING/MONITORING AGENCY NAME(S) AND ADDRESS(ES) U.S. Army Research Laboratory 2800 Powder Mill Road Adelphi, MD 20783-1145		10. SPONSORING/MONITORING AGENCY REPORT NUMBER ARL-TR-1733	
11. SUPPLEMENTARY NOTES			
12a. DISTRIBUTION/AVAILABILITY STATEMENT Approved for public release; distribution unlimited.		12b. DISTRIBUTION CODE A	
13. ABSTRACT (Maximum 200 words) Under realistic conditions, helicopters are exposed to electromagnetic (EM) radiation from friendly and hostile sources. The radiating source is sufficiently far away that the helicopter is in the far field of the source antenna and plane wave conditions apply. To determine how the systems and subsystems on board the helicopter are affected by electromagnetic environment effects (E ³), the tests are normally performed under controlled laboratory or controlled field conditions. The tests are performed with the test object in the near field rather than in the far field zone of the source antenna. The helicopter under test is "spot" illuminated instead of being totally illuminated by plane waves. This report provides an understanding of the magnitude of the uncertainties incurred when E ³ tests are performed in the near field rather than plane wave environment.			
14. SUBJECT TERMS electromagnetic effects, near field, far field, EMV		15. NUMBER OF PAGES 59	
		16. PRICE CODE	
17. SECURITY CLASSIFICATION OF THIS REPORT UNCLASSIFIED	18. SECURITY CLASSIFICATION OF THIS PAGE UNCLASSIFIED	19. SECURITY CLASSIFICATION OF ABSTRACT UNCLASSIFIED	20. LIMITATION OF ABSTRACT SAR

Preface

The purpose of this report is to document the results of an assessment of the Longbow Apache AH-64D electromagnetic environmental effects (E³) program, to set forth the E³ issues that remain to be resolved, and to present a Survivability/Lethality Analysis Directorate, Information & Electronic Protection Division plan for U.S. Army Research Laboratory's monitoring of First Article E³ tests.

Contents

Preface	1
Executive Summary	5
1. Introduction	7
2. Objective	9
3. Methodology	11
3.1 <i>First Investigation</i>	11
3.1.1 Methodology	11
3.1.2 Results	11
3.2 <i>Second Investigation</i>	12
3.2.1 Methodology	12
3.2.2 Results and Analyses	14
4. Conclusions	41
5. Additional Discussions	43
References	47
Acronyms and Abbreviations	49
Distribution	51

Figures

1. Mock missile with a nose-mounted thin-wire probe	13
2. Geometry: Dipole located at $(x_c, 0, z_c)$, displaced along a line parallel to z-axis	15
3. Voltage plots: Single z-directed dipole displaced along z direction with a fixed ρ location	17
4. Voltage plots: Single z-directed dipole varied along z direction with a fixed ρ location (larger distance away from the body)	18
5. Geometry: Dipole located at $(x_c, 0, z_c)$, displaced along a straight line in the x-z plane and its height is constant	20
6. Voltage plots: Single z-directed dipole displaced along ρ direction with a fixed z (negative) location	21

7. Voltage plots: Single z-directed dipole displaced along ρ direction with a fixed z (positive) location	.22
8. Geometry: Line source of $\lambda/2$ length centered at $(x_c, 0, z_c)$ and is displaced along a line parallel to the z -axis	.23
9. Voltage plots: z -directed line source (represented by 11 unity strength dipoles) displaced along z direction with a fixed ρ location	.25
10. Geometry: Line source of $\lambda/2$ length centered at $(x_c, 0, z_c)$ and is displaced along a line in the x - z plane. Its height is constant	.26
11. Voltage plots: z -directed line source of $\lambda/2$ length (represented by 11 unity strength dipoles). The line source is varied along ρ direction with a fixed z location	.27
12. Geometry: 4 by 4 dipole array centered at $(x_c, 0, z_c)$ and located on x - z plane. The array is displaced along a line parallel to the z -axis and its distance to the z -axis is constant	.29
13. Voltage plots: Sheet current represented as 4 by 4 dipole array displaced along z -axis with a fixed ρ location	.30
14. Geometry: 4 by 4 dipole array centered at $(x_c, 0, z_c)$ and located on the x - z plane. It is displaced along a line in the x - z plane and its z position is constant	.32
15. Voltage plots: Sheet current represented as 4 by 4 dipole array varied along ρ direction with a fixed z location	.33
16. Geometry: 4 by 4 dipole array centered at $(x_c, 0, z_c)$ and is parallel to y - z plane. It is displaced along a line parallel to the x -axis and z_c is constant.	.35
17. Voltage plots: Sheet current represented as 4 by 4 dipole array parallel to y - z plane, displaced along z direction	.36
18. Geometry: 4 by 4 dipole array centered at $(x_c, 0, z_c)$ and is parallel to y - z plane. It is displayed along a line parallel to the z -axis and x_c is constant	.38
19. Voltage plots: Sheet current represented as 4 by 4 dipole array parallel to y - z plane, displaced along ρ direction with a fixed z	.39
20. Geometry for determining uniform EM field illumination	.44

Executive Summary

Introduction

Under real world conditions, helicopters (in storage, while being transported, in standby mode, or in operation) are often exposed to electromagnetic (EM) radiation from friendly and hostile sources. Typically, the radiating source is sufficiently far away that the helicopter is in the far field of the source and plane wave conditions apply. To determine how the systems and subsystems onboard the helicopter are affected by exposure to these EM sources, it is necessary to test them under EM environment (EME) conditions different from the real world. This is because the available sources are limited in power capabilities. In addition, for safety reasons it is desirable to subject the helicopter to the sources while on the ground in case deleterious effects occur. EM vulnerability (EMV) investigations are normally performed under controlled laboratory or controlled field conditions. Under these conditions, the tests are performed with the test object in the near field rather than in the far field zone of the source antenna. The helicopter under test is "spot" illuminated instead of being subjected to total target illumination by plane waves that occur under real world conditions.

Objective

The objective of this report is to determine and quantify the difference in the response of the onboard systems/subsystems when the helicopter is totally illuminated by impinging plane waves as opposed to when the helicopter is "spot" illuminated by a source operating in the near field zone.

Methodology

This report is based on two theoretical investigations. The first investigation determined the magnitude of the effects on the onboard systems/subsystems by theoretically computing the skin or surface currents induced on the test object and then validating these with measurements. The target was a thin cylindrical rod or wire. To assess the effects of near field source, the surface currents on the thin wire were calculated for several frequencies as the source distance from the target was varied. The incident field was kept constant at 1 V/m. Therefore, the differences in the results obtained are due strictly to the field complexities

that occur in the near field and the effects of the $1/R$ distance factor are eliminated.

The second investigation addressed a mock missile with a nose-mounted thin-wire probe. The wire probe was connected to a load Z_L . The received signal was across the load impedance. In the analyses, full account was taken of the coupling among the wire, the missile body proper, and the load impedance. Of significant importance in this second investigation is that the voltage across the impedance load, inside the mock missile, was calculated. It is possible or even more probable that a more directive source would produce greater discrepancies when the test object is in the near field than are found for the different configurations of dipole sources considered in this investigation. The voltage across the impedance load, resulting from excitation of the probe at the top of the mock missile, is due to the integrated effect of the incident field along the entire length of the missile. As the source is moved closer to, or further from the mock missile, the field intensity and phase distribution change along the missile because of geometry changes. A measure of the magnitude of the errors that can occur is achieved by comparing the ratio of the voltages across the impedance load at near- and far field ranges with the ratio that can be expected to occur because of the $1/R$ change in field strength ($1/R$ distance factor) under plane wave conditions.

Conclusions

The results of the two theoretical investigations provide an understanding of the magnitude of the uncertainties when E^3 tests are performed in near field rather than plane wave environments.

Applying the results of the two theoretical investigations to the E^3 tests, it appears that near field testing, when compared to far field testing, can be in error due to near field complexities by as much as 6 dB and possibly more for more complex sources and test objects. Near field predictions are always lower than far field predictions as seen in both theoretical investigations.

1. Introduction

Under real world conditions, helicopters (in storage, while being transported, in standby mode, or in operation) are often exposed to electromagnetic (EM) radiation from friendly and hostile sources. Typically, the radiating source is sufficiently far away that the helicopter is in the far field of the source and plane wave conditions apply. To determine how the systems and subsystems onboard the helicopter are affected by exposure to these EM sources, it is necessary to test them under EM environment (EME) conditions different from the real world. This is due to power limitations of available sources. Also, for safety reasons it is desirable to subject the helicopter to the sources while on the ground in case deleterious effects occur. EM vulnerability (EMV) investigations are normally performed under controlled laboratory or controlled field conditions. Under these conditions, the tests occur with the test object in the near field rather than in the far field zone of the source antenna. To produce the real world threat power density levels and broad frequency ranges, tests are performed with the helicopter in the near field zone of the source. The helicopter under test is "spot" illuminated instead of being subjected to total target illumination by plane waves that occur under real world conditions.

2. Objective

The objective of this report is to determine and quantify the difference in the response of the onboard systems/subsystems when the helicopter is totally illuminated by impinging plane waves, as opposed to when the helicopter is "spot" illuminated by a source operating in the near field zone.

3. Methodology

This study is based on two theoretical investigations: *Some Aspect of Valid EMC Testing of Missiles* and *Complex Near Source Coupling to Probe on Mock Missile*. [1,2]

3.1 First Investigation

3.1.1 Methodology

In the first investigation, the magnitude of the effects on the onboard system/subsystems is determined by theoretically computing the skin or surface currents induced on the target and then validating these with measurements. [1] This investigation employed the thin-wire theory using integral equations and the method of moments. The target was viewed as a thin cylindrical rod (length \gg diameter). The assumption was made that the skin currents are rotationally symmetric and flow only in the axial direction. Only the zeroth mode axial current was determined. To assess the effects of near field source, the surface currents on the thin wire were calculated for several frequencies as the source distance from the target was varied. Incidence angle was also varied. The incident field was kept constant at 1 V/m. Therefore, the differences in the results obtained are due strictly to the field complexities that occur in the near field and the effects of the $1/R$ distance factor are eliminated.

3.1.2 Results

Results of the first investigation show that a factor of two difference can exist in the skin currents induced by the source operating at near field versus when the source is at far field. This occurred for broadside incidence. This difference in skin currents equates to a 6 dB difference in power that can occur when the source is operating in the near field zone. For this particular geometry and test object (thin cylinder), an incident field of 2 V/m would be required from a near field source to produce the same effects as a 1 V/m plane wave field.

NOTE: The skin current creates the fields that can penetrate through apertures in the target skin into the interior of the target and can affect the performance of the onboard systems/subsystems. The most crucial issue of a target's vulnerability to an EME is the coupling of the generated fields into the interior of the target. Schelkunoff derived the equivalence theorem which states that, to

find internal fields in targets that contain apertures and are illuminated by external sources, one may replace the problem by an equivalent condition having only aperture current sources for excitation. [3] In addition, the aperture currents to be used are precisely the negative of those that would be generated on the target if the apertures were short circuited. NOTE: The aperture current is nothing more than the surface or skin current produced on the "solid" cylindrical rod (equates to target with apertures short circuited). This equivalence theorem establishes the direct relationship of the coupling analysis pertaining to targets containing apertures and the solid-body or cylindrical rod analysis.

3.2 Second Investigation

3.2.1 Methodology

The second theoretical investigation involves a mock missile with a nose-mounted, thin-wire probe. [2] In the case of an actual system, the probe is connected to some component inside the missile body. In this particular case, the probe is connected to a load Z_L as figure 1 shows. (All figures in this report are derived from the *Complex Near Source Coupling To Probe on Mock Missile* theoretical investigation.) [2] The wire probe is connected to the center conductor of a coaxial cable that extends into the body of the mock missile. The received signal is that across the load impedance at the end of the coax. The analysis is based upon the integral equation theory, leading to equations that are solved by numerical (computer) methods. In the analyses, a full account is taken of the coupling among the wire, the missile body proper, and the load impedance at the end of the coax. Of significant importance in this second investigation is the fact that the voltage across the impedance load, inside the mock missile, was calculated.

The *Complex Near Source Coupling to Probe on Mock Missile* theoretical investigation is used in this E^3 study to gain an understanding of the differences that can occur in internal system response when the test missile is in the far field of the radiating source and when in the near field. [2] The internal components' responses will be directly proportional to the voltage across the impedance load located inside the mock missile.

It is, of course, possible or even probable that a more directive source would produce greater discrepancies when the test object is in the near field than are found for the dipole sources considered in this investigation. However, the results for this simple configuration can help to provide an understanding of the magnitude of the uncertainties when E^3 tests are performed in near field rather than plane wave environments.

3.2.2 Results and Analyses

In the following analyses, a comparison is made between the voltage across the impedance load when the mock missile is in the near field of the source and the voltage across the impedance load when the source is far enough away that the field at the missile is essentially a plane wave. The change in the voltage across the impedance load for these two different test conditions is due to two effects. One effect is the reduction in field strength at the mock missile when the source is moved farther away. The radiation field intensity from a dipole source falls off as $1/R$ with distance R from the dipole and has a cosine θ antenna pattern. The second effect is due to differences in field distribution between near field and far field conditions. The voltage across the impedance load, resulting from excitation of the probe at the top of the mock missile, is due to the integrated effect of the incident field along the entire length of the missile. As the source is moved closer to, or farther from the mock missile, the field intensity and phase distribution change along the missile because of geometry changes. For example, when the source is very close to the center of the missile, a greater relative change in intensity and phase will occur along the length of the mock missile than when the source is far removed from the missile. The second effect occurs only when the test object (mock missile in this case) is close to (in the near field of) the source.

This second effect can lead to errors in E^3 test results if a specified test field intensity is achieved by bringing the source antenna close to the test object (helicopter in the E^3 test) rather than maintaining the antenna at an appropriate range (far field) and increasing the transmitter power. Increasing the transmitter power was not possible in the E^3 tests because of the limitations in power of the available sources.

In the following analyses, a measure of the magnitude of the errors that can occur is achieved by comparing the ratio of the voltages across the impedance load at near- and far field ranges with the ratio that could be expected to occur just due to the $1/R$ change in field strength ($1/R$ distance factor) under plane

wave conditions. In order to express these ratios in decibels (dB), the ratio of the squares of the voltages across the impedance load is compared with the $1/R^2$ change in electric field power density (electric field squared).

The data presented are for 100 MHz. The wavelength (λ) is 3 m at 100 MHz. The following conditions are addressed:

Condition 1 Excitation Source: one unity strength z-directed dipole. The dipole is located at $(x_c, 0, z_c)$ as figure 2 shows. The dipole is displaced along a line parallel to the z-axis. The dipole's distance from the z-axis is constant (x_c or ρ_c is fixed).

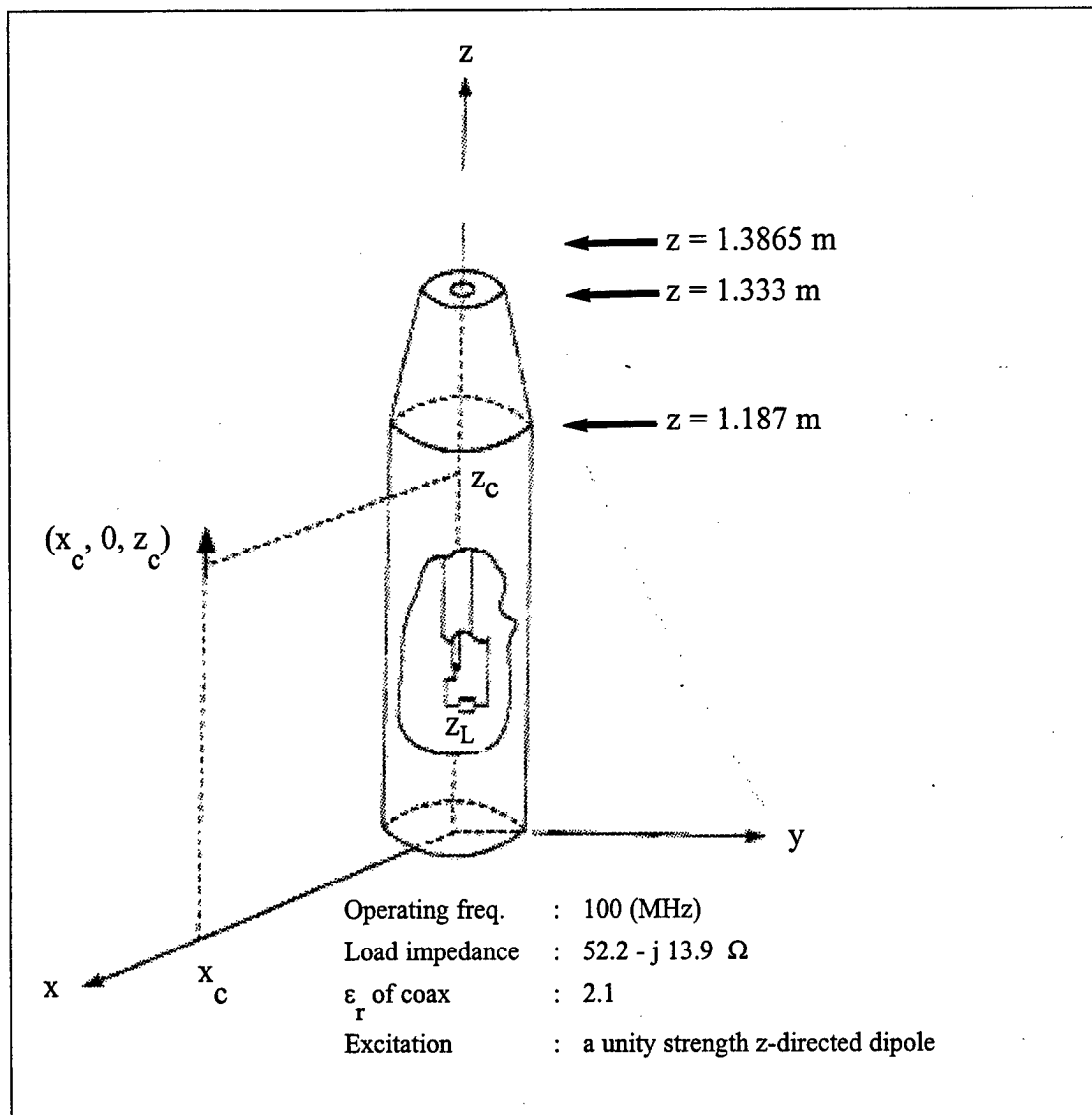


Figure 2. Geometry: Dipole located at $(x_c, 0, z_c)$, displaced along a line parallel to z-axis.

Various values of fixed ρ_c are plotted, starting from a distance (from the mock missile) of $\lambda/10$ to 5λ . NOTE: The radius of the mock missile is b . Therefore, the dipole is moved from $x_c = b + \lambda/10$ to $x_c = b + 5\lambda$. Figures 3 and 4 show the voltage across the load impedance versus the dipole's position along the z-axis direction with different fixed ρ_c . (ρ_c is the dipole distance from the z-axis of the mock missile.)

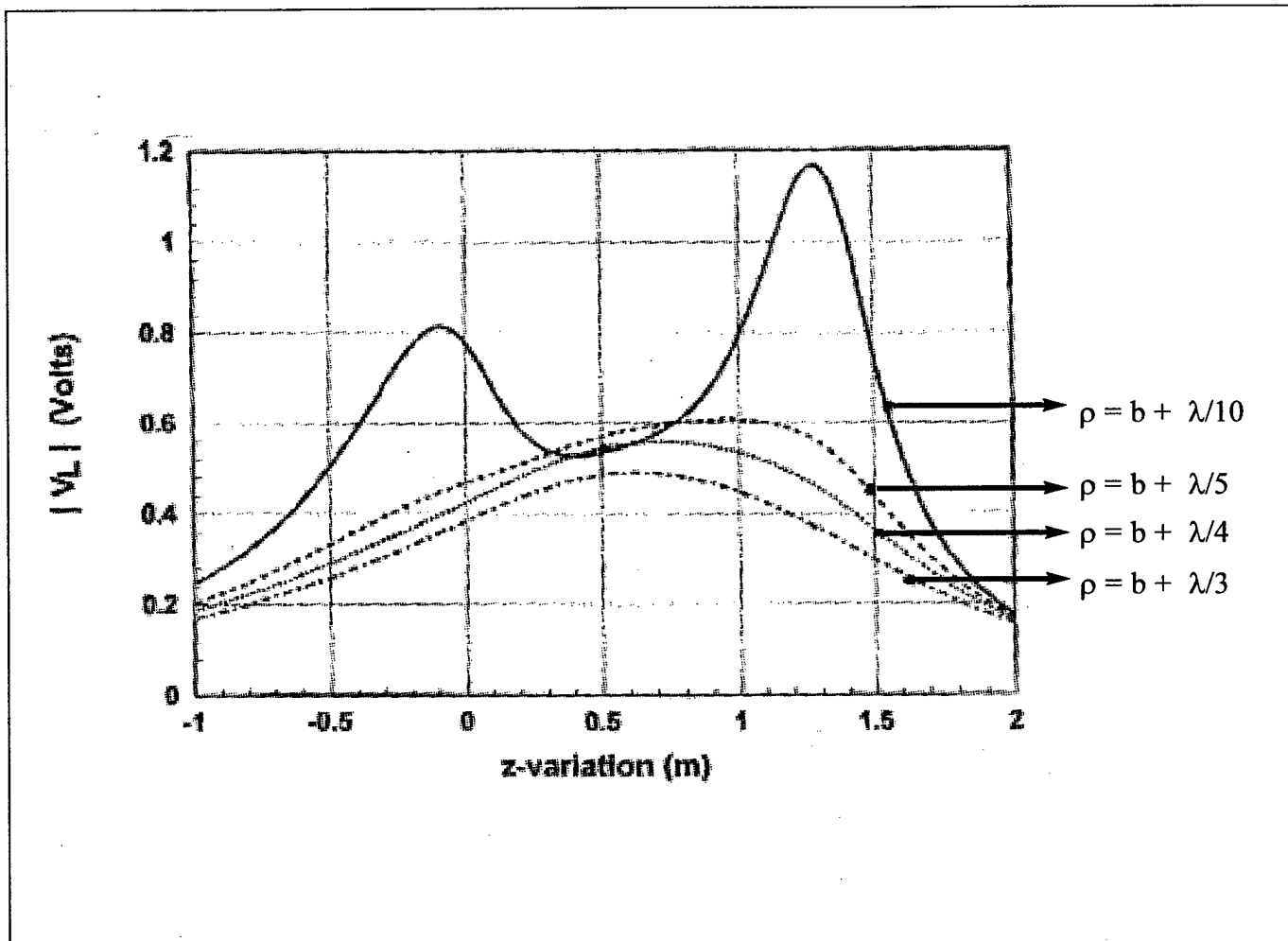


Figure 3. Voltage plots: Single z -directed dipole displaced along z direction with a fixed ρ location.

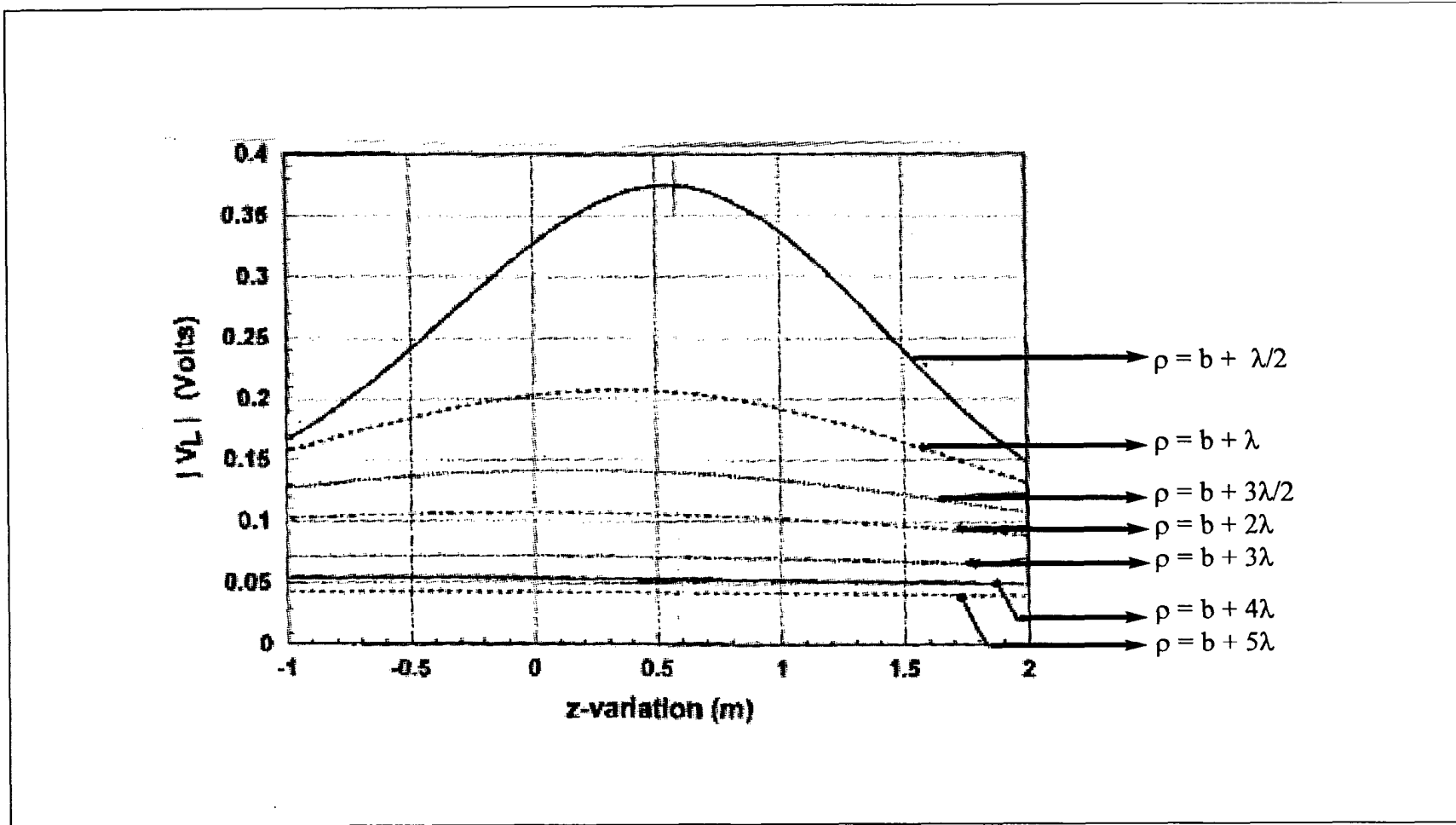


Figure 4. Voltage plots: Single z -directed dipole varied along z direction with a fixed ρ location (larger distance away from the body).

Condition 1 Analysis: as figure 2 shows, the mock missile's cylindrical section has a midheight of 0.594 m ($z = 0.594$ m). Figure 4 shows that the voltage across the impedance load (at $z = 0.594$ m) is 0.375 V when the dipole is positioned at $x_c = b + \lambda/2$ from the mock missile's axis. Voltage across the impedance load (at $z_c = 0.594$ m) is 0.052 V when the dipole is positioned at $x_c = b + 4\lambda$. This is a change of 17.2 dB (due to change in dipole source position from near field to far field). However, this voltage change is mostly due to the $1/R^2$ distance factor as range is increased from near field to far field. Computed change due strictly to the $1/R^2$ factor is 18.06 dB. The radius (b) of the mock missile is less than the missile length and is less than the wavelength (λ). Range at $\lambda/2 = 1.5$ m. Range at $4\lambda = 12$ m. The change expected due to the increase in range as the dipole was moved from near field to far field is 18.06 dB.

In this case and selected conditions, it appears that the effect from near field to far field is all due to the $1/R^2$ factor and nothing due to the circularity of the impinging wave and other complexities that occur at the near field zone. Further investigation of the plots in figure 4 show that as one moves away from either side of the missile midpoint in the z -axis, the dB change across the impedance load further decreases when going from near field to far field.

The distance R of the source from the test object, where the far field begins is that value of R for which the path length deviation (from the nearest to the farthest point on the test object as measured from the source) is a sixteenth of a wavelength. This corresponds to a phase error of $2\pi/\lambda$ multiplied by $\lambda/16 = \pi/8$ radian or 22.5° . This far field requirement is satisfied when the distance R from the source to the test object is $R > 2d^2/\lambda$ (where d is the significant dimension of either the source or the test object, whichever is the largest). In this case, d is the length of the mock missile and is 1.3865 m. Wavelength $\lambda = 3$ m. To satisfy the far field condition, R should be greater than $2d^2/\lambda = 1.28$ m. For condition 1, the dipole source position moved from $(b + \lambda/2)$ to $(b + 4\lambda)$.

Condition 2 Excitation Source: one unity strength z -directed dipole. The dipole is located at $(x_c, 0, z_c)$ as figure 5 shows. The dipole is displaced along a straight line in the x - z plane and the distance from the missile axis is varied (ρ_c is varied). The dipole distance from the x - y plane is constant (z_c is fixed). Various plots of the voltage across the impedance load versus dipole distance (ρ_c) from the mock missile, for fixed z_c , are shown in figures 6 and 7.

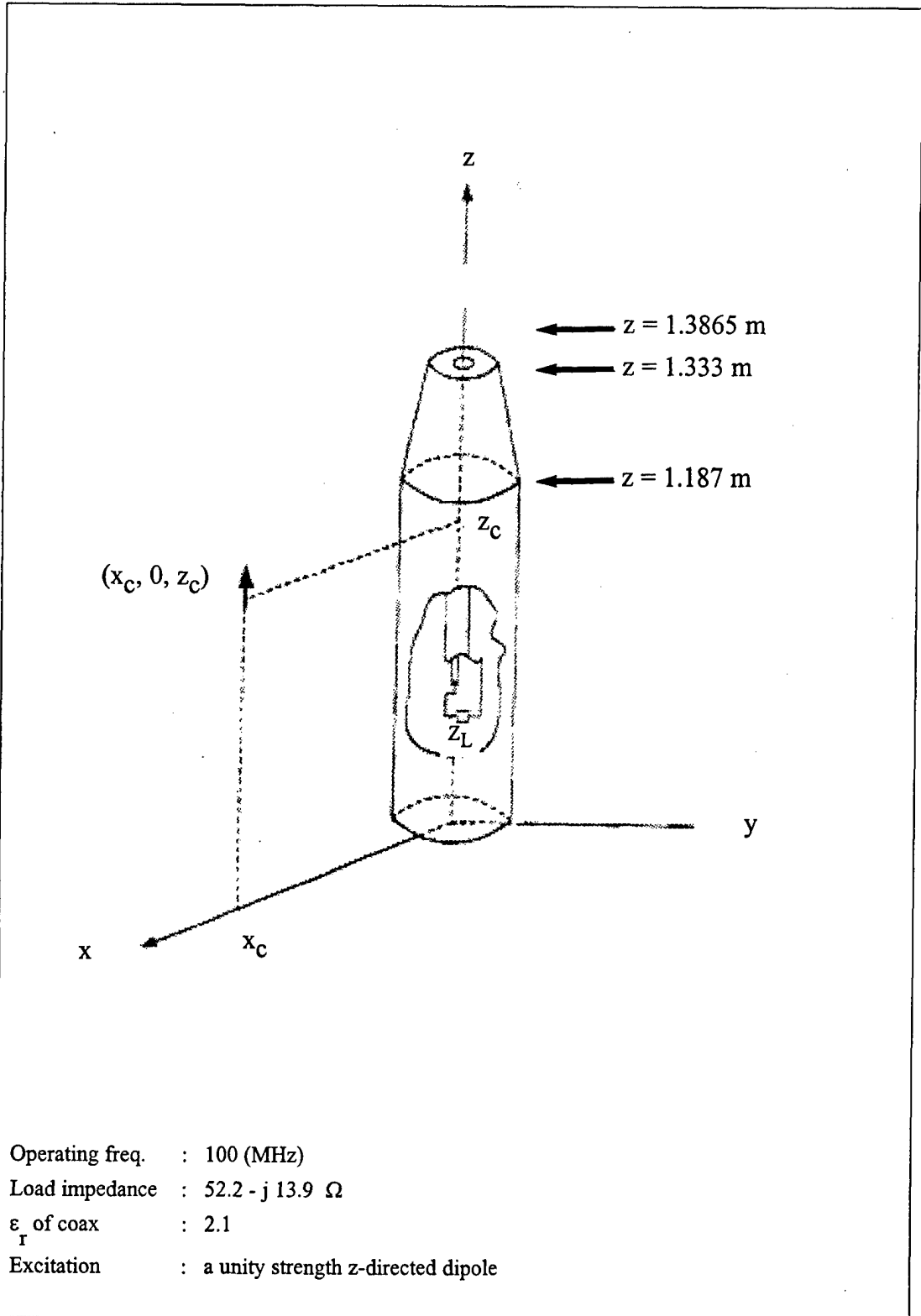


Figure 5. Geometry: Dipole located at $(x_c, 0, z_c)$, displaced along a straight line in the x-z plane and its height is constant.

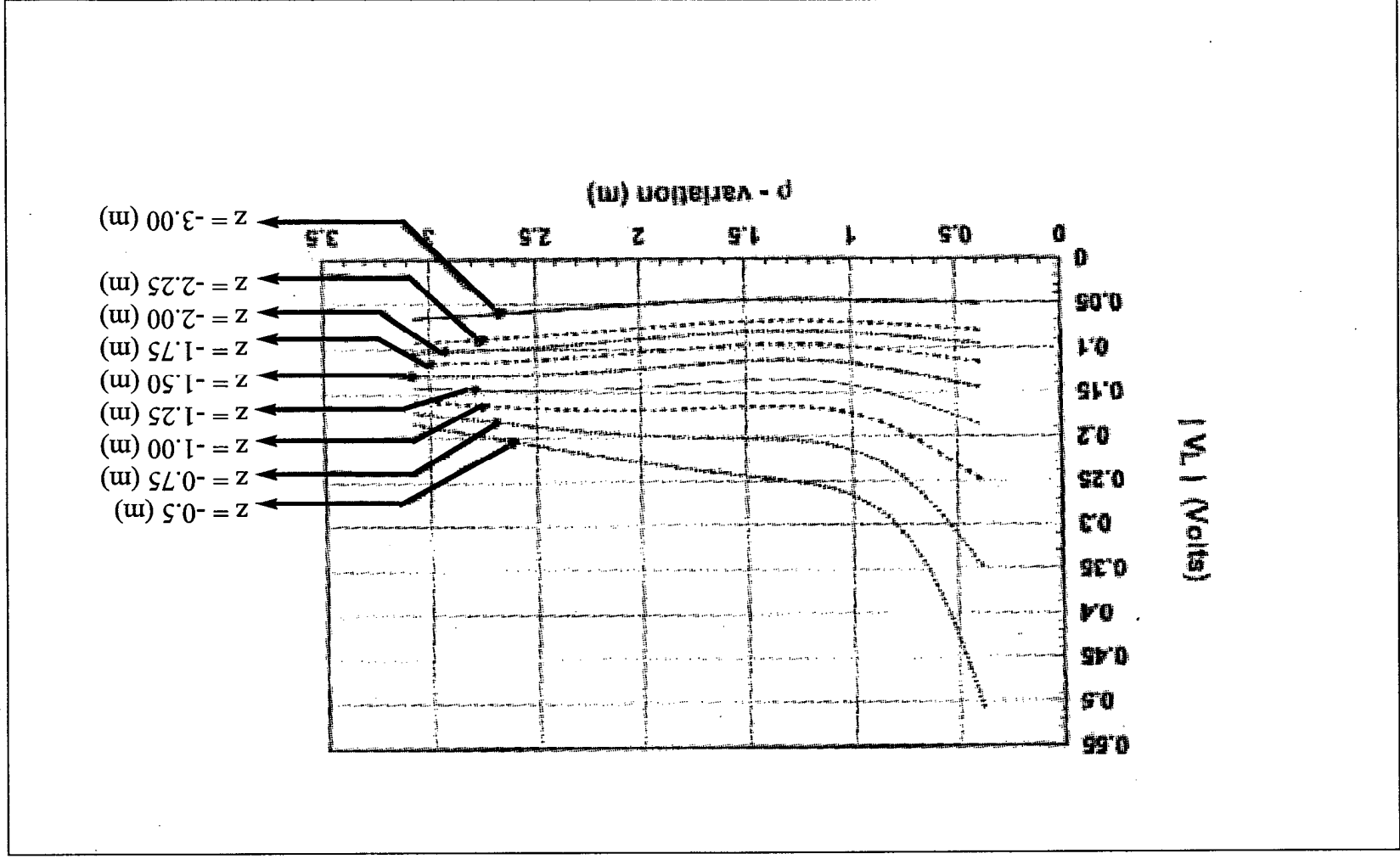


Figure 6. Voltage plots: Single z-directed dipole displaced along p direction with a fixed z (negative) location.

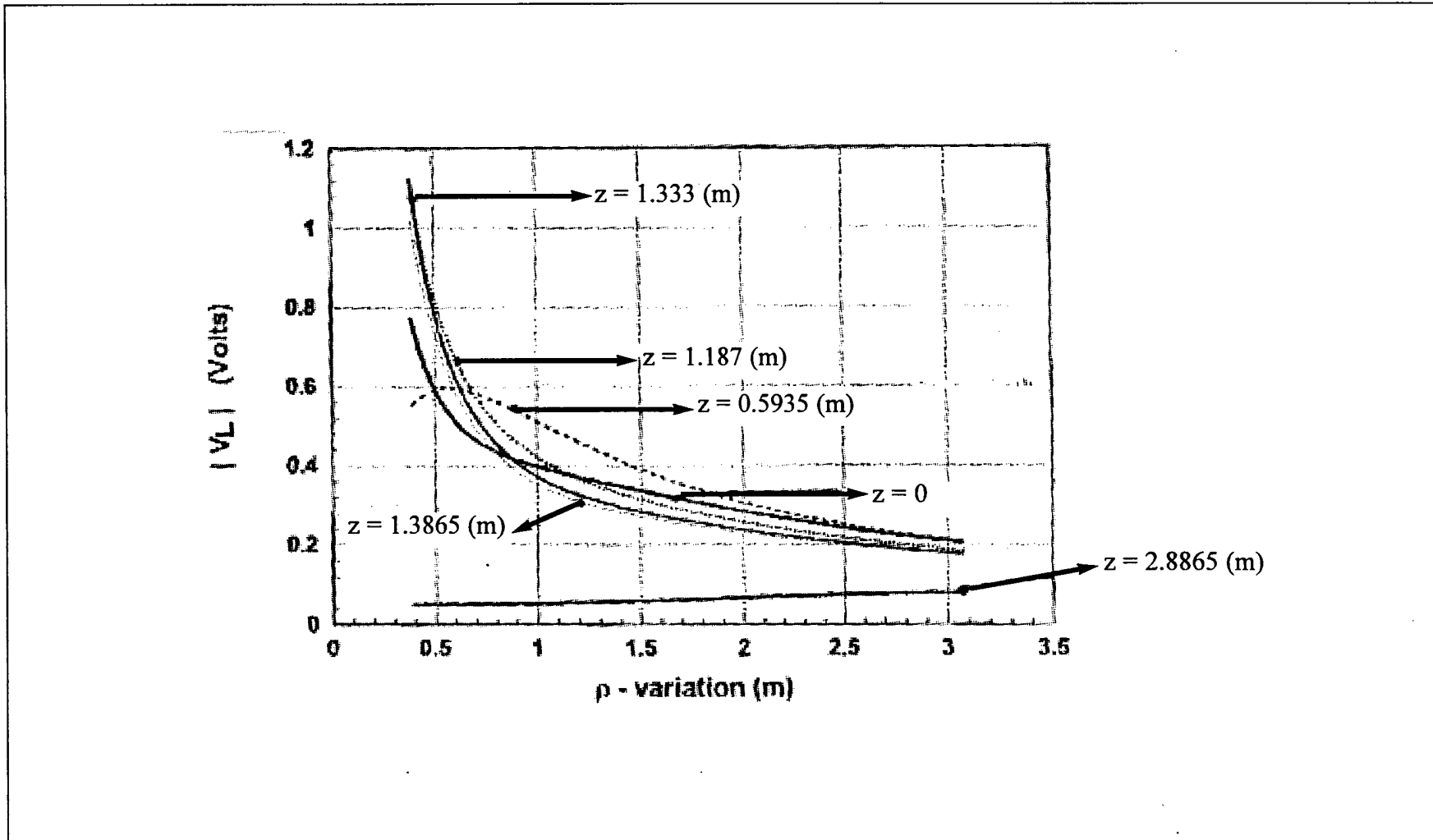


Figure 7. Voltage plots: Single z -directed dipole displaced along ρ direction with a fixed z (positive) location.

Condition 2 Analysis: as figure 5 shows, the mock missile's cylindrical section has a midheight of 0.594 m ($z_c = 0.594$ m). As figure 7 shows, the voltage across the impedance load is 0.6 V when the dipole distance from the mock missile is $\rho_c = 0.6$ m. The voltage across the impedance load is 0.2 V when the dipole distance from the mock missile is $\rho_c = 3.1$ m. This is a change of 9.54 dB from moving the dipole position away from the missile axis ($\rho_c = 0.6$ m to $\rho_c = 3.1$ m). The source dipole is at a height of $z_c = 0.594$ m. The expected change due to moving away in range ($1/R^2$ distance factor) is 14.2 dB. This is considerably more than the change observed in the voltage across the impedance load.

Condition 3 Excitation Source: the line source of $\lambda/2$ length is represented by 11 unity strength z directed dipoles. The line source is centered at $(x_c, 0, z_c)$. As figure 8 shows, the line source is displaced along a line parallel to the z-axis and the line source's distance from the z-axis is constant (x_c or ρ_c is fixed). Plots of the voltage across the impedance load versus line source height along the line parallel to the z-axis with fixed ρ_c are shown in figure 9. The distance from the mock missile axis was varied from $x_c = b + \lambda/5$ to $x_c = b + 2\lambda$. NOTE: The radius of the mock missile is b and x_c and ρ_c are interchangeable or equivalent.

Condition 3 Analysis: as figure 8 shows, the excitation source is a line source of $\lambda/2$ length, represented by 11 unity strength z directed dipoles. The mock missile's cylindrical section has a midheight of 0.594 m ($z_c = 0.594$ m). As figure 9 shows, the voltage across the impedance load is 4 V when the line source distance from the mock missile is $\rho_c = b + \lambda/2$ or ≈ 1.5 m. The voltage across the impedance load is 1.2 V when the line source distance from the mock missile is $\rho_c = b + 2\lambda$ or ≈ 6 m. The line source is at a height of $z_c = 0.594$ m. This is a change of 10.46 dB from moving the line source position away from the missile axis ($\rho_c = 1.5$ m to $\rho_c = 6$ m). The expected change due to moving away in range ($1/R^2$ distance factor) is 12.04 dB. This is ≈ 1.58 dB more than the change observed in the voltage across the impedance load. Referring back to condition 1, the mock missile was in the far field of the line source in both positions of the source.

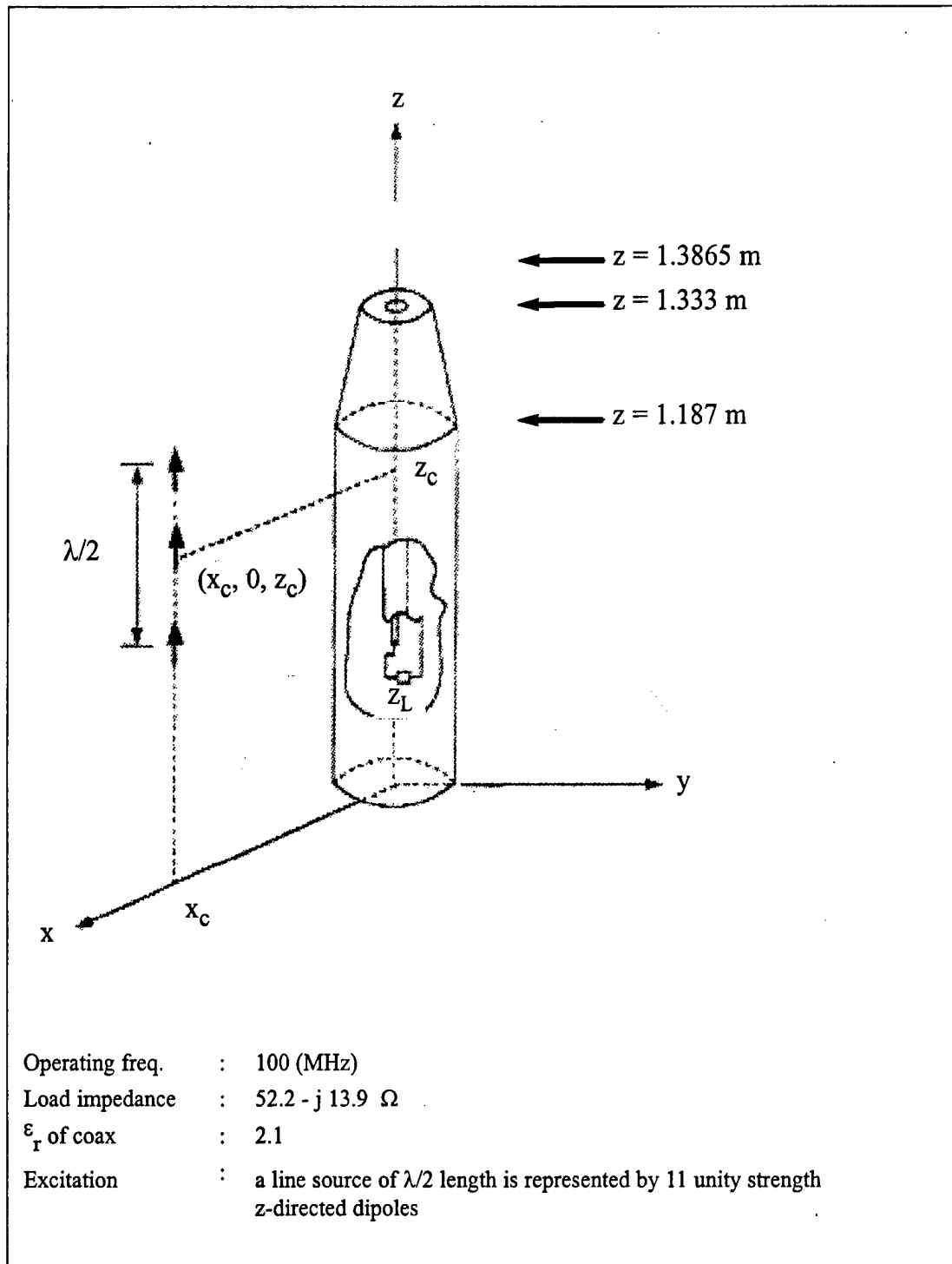


Figure 8. Geometry: Line source of $\lambda/2$ length centered at $(x_c, 0, z_c)$ and is displaced along a line parallel to the z-axis.

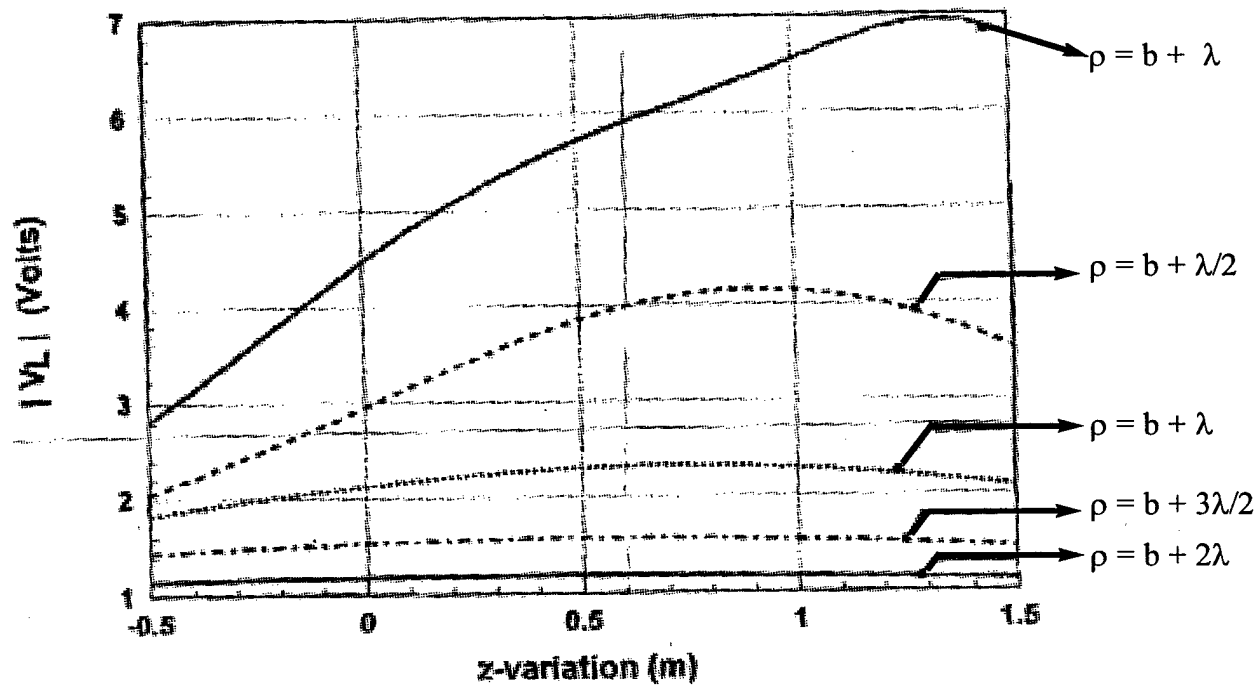


Figure 9. Voltage plots: z-directed line source (represented by 11 unity strength dipoles) displaced along z direction with a fixed ρ location.

Condition 4 Excitation Source: the line source of $\lambda/2$ length is represented by 11 unity strength z-directed dipoles. The line source is centered at $(x_c, 0, z_c)$. As figure 10 shows, the line source is displaced along a line in the x-z plane and its height is constant (z_c is fixed). Plots of the voltage across the impedance load versus line source's distance from the mock missile (ρ_c is varied from ≈ 0.35 to 2.9 m) are shown in figure 11.

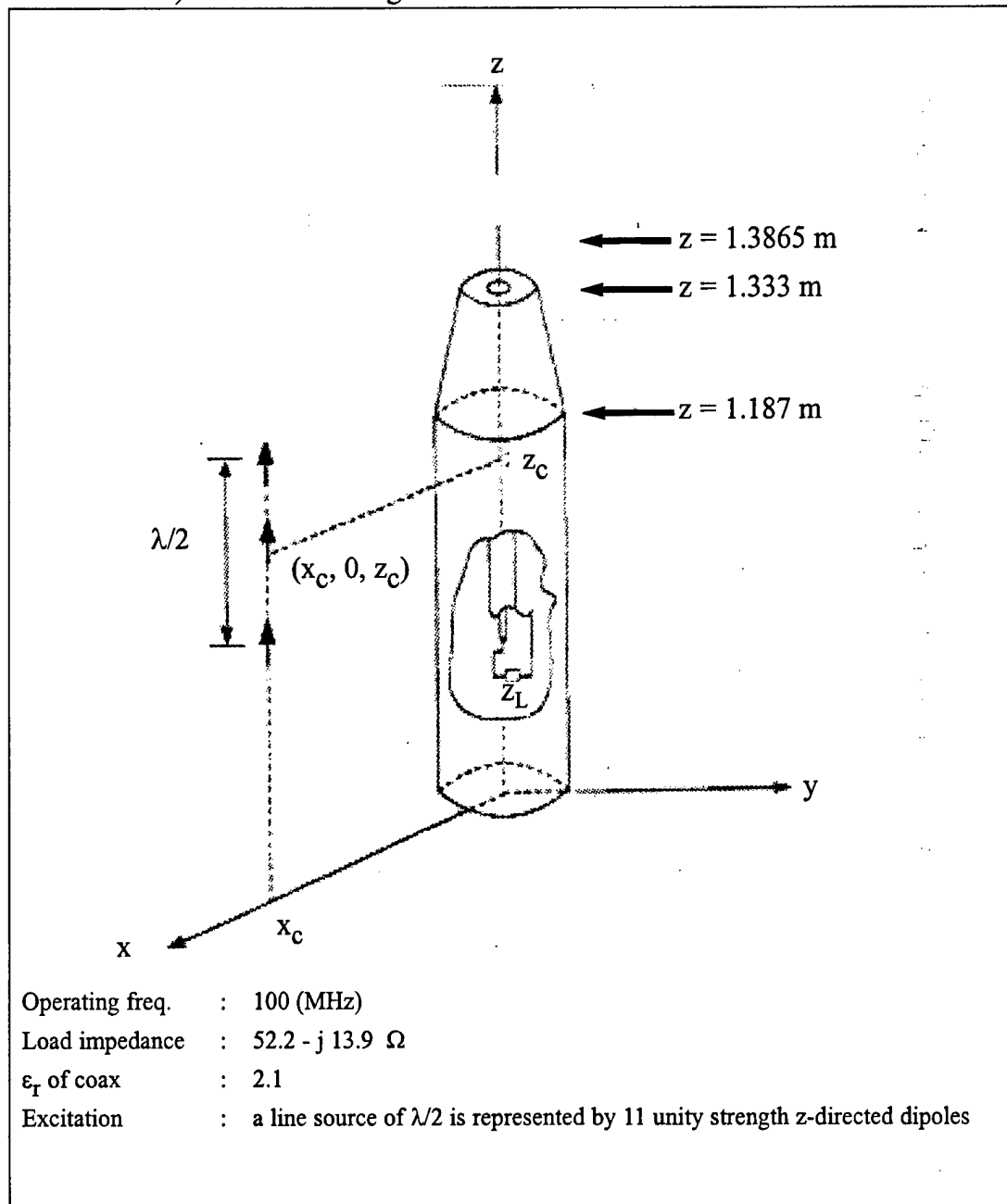


Figure 10. Geometry: Line source of $\lambda/2$ length centered at $(x_c, 0, z_c)$ and is displaced along a line in the x-z plane. Its height is constant.

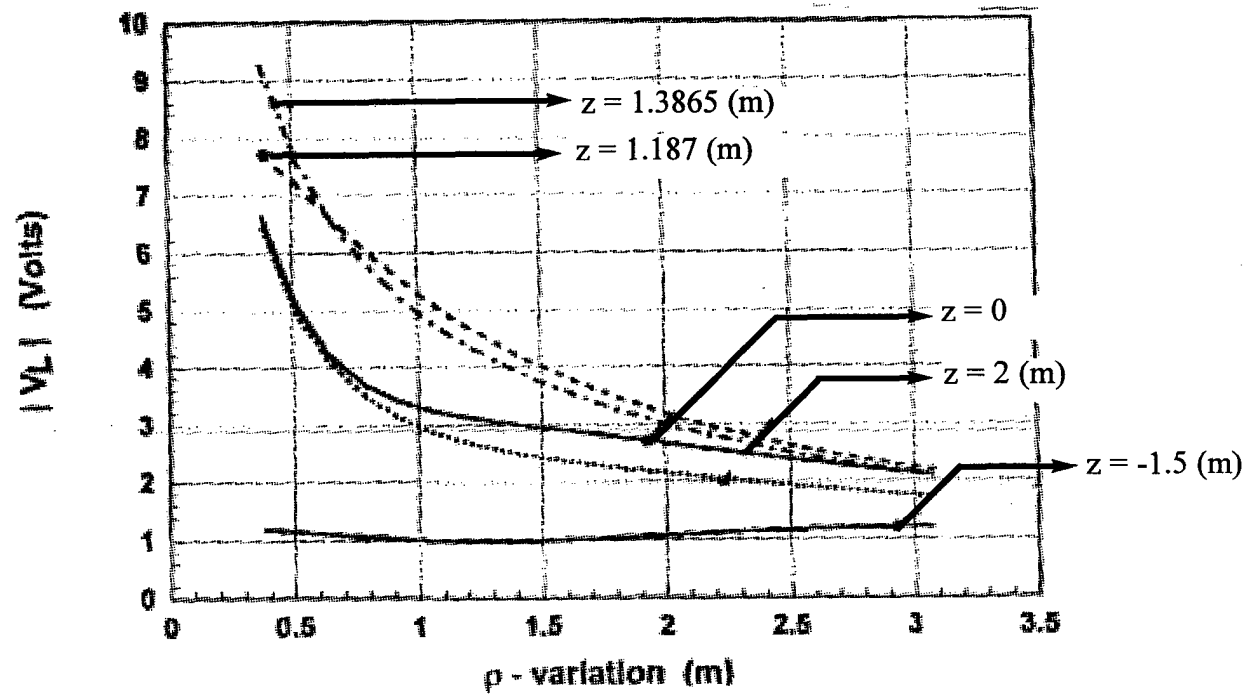
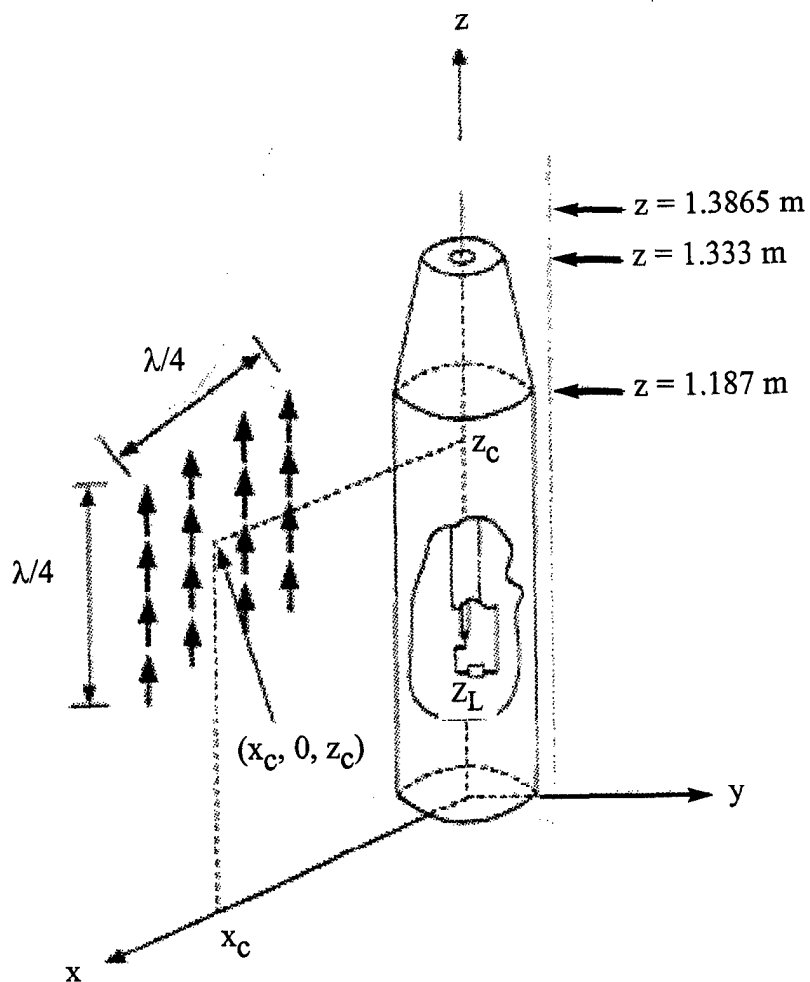


Figure 11. Voltage plots: z -directed line source of $\lambda/2$ length (represented by 11 unity strength dipoles). The line source is varied along ρ direction with a fixed z location.

Condition 4 Analysis: as figure 10 shows, the excitation source is a line source of $\lambda/2$ length, represented by 11 unity strength z-directed dipoles. The mock missile has a tapered cone on top of the cylindrical section. This taper starts at $z_c = 1.187$ m along the z-axis. The line source is at a height of $z_c = 1.187$ m (where the taper of the cone begins). As figure 11 shows, the voltage across the impedance load is 7.6 V when the line source distance from the mock missile is $\rho_c = 0.4$ m. The voltage across the impedance load is 2.1 V when the line source distance from the mock missile is $\rho_c = 3.1$ m. This is a change of 11.18 dB due to moving the line source position further away from the missile axis ($\rho_c = 0.4$ m to $\rho_c = 3.1$ m). The expected change due to moving away in range ($1/R^2$ distance factor) is 17.78 dB. This is more than the change observed in the voltage across the impedance load. NOTE: The line source height was not at the middle of the missile's cylindrical section. We observed previously that illuminating the missile at this midpoint produced the largest change in voltage across the impedance load.

Condition 5 Excitation Source: 4 by 4 dipole array (sheet of current on x-z plane represented by 4 by 4 unity strength z-directed dipole array). The 4 by 4 dipole array is centered at $(x_c, 0, z_c)$ and located on the x-z plane. As figure 12 shows, the dipole array is displaced along a line parallel to the z-axis and the array's distance from the z-axis is constant (x_c is fixed). Plots of the voltage across the impedance load versus array height along the line parallel to the z-axis with fixed ρ_c are shown in figure 13. The distance from the mock missile axis was varied from $x_c = b + \lambda/2$ to $x_c = b + 2\lambda$. NOTE: The radius of the mock missile is b and x_c and ρ_c are equivalent.



Operating freq. : 100 (MHz)
 Load impedance : $52.2 - j 13.9 \Omega$
 ϵ_r of coax : 2.1
 Excitation : a sheet of current on x - z plane is represented by 4 by 4 unity strength z -directed dipole array.

Figure 12. Geometry: 4 by 4 dipole array centered at $(x_c, 0, z_c)$ and located on x - z plane. The array is displaced along a line parallel to the z -axis and its distance to the z -axis is constant.

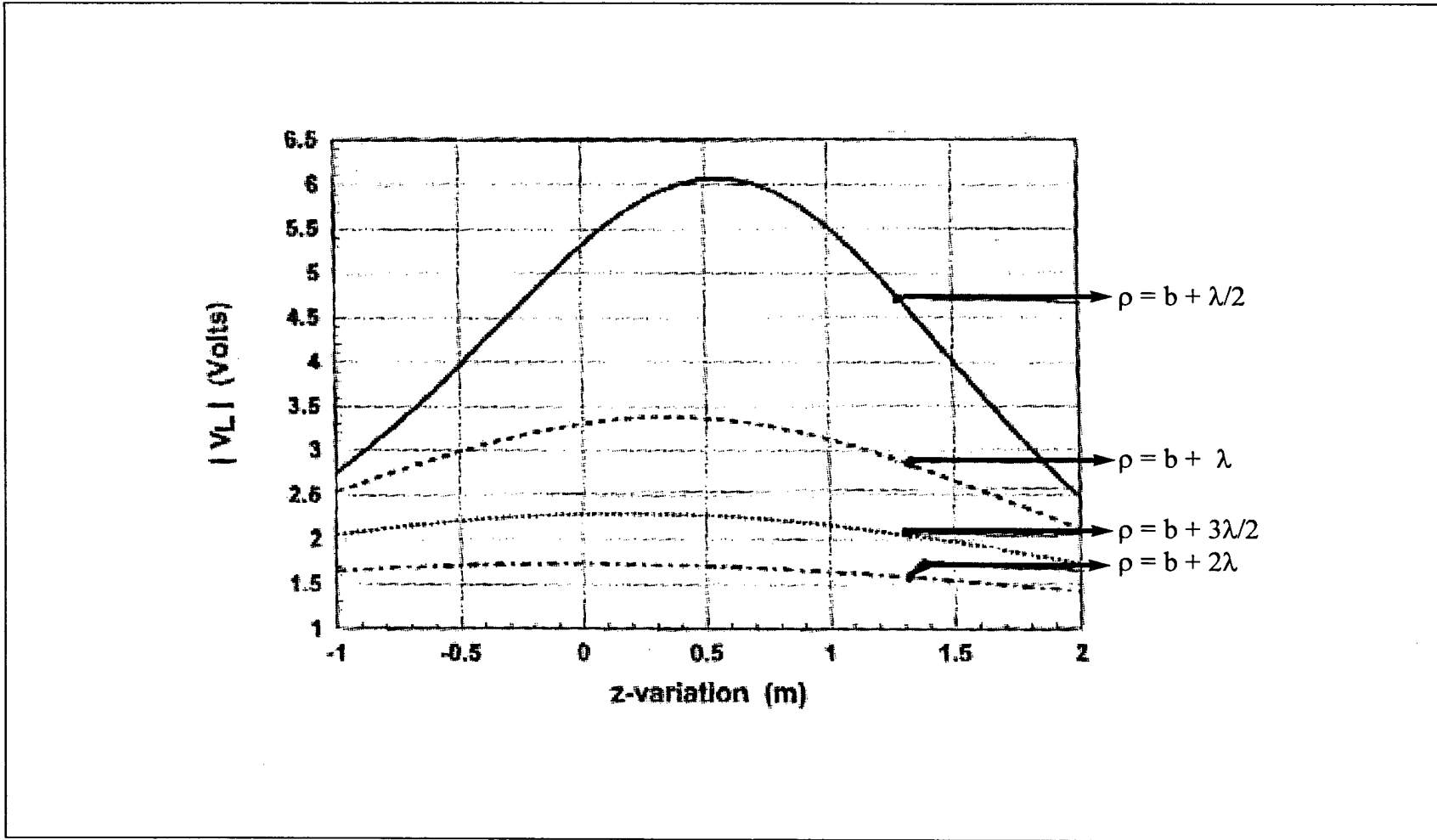


Figure 13. Voltage plots: Sheet current represented as 4 by 4 dipole array displaced along z -axis with a fixed ρ location.

Condition 5 Analysis: as figure 12 shows, the excitation source is a 4 by 4 dipole array (sheet of current on the x-z plane represented by a 4 by 4 unity strength z-directed dipole array). The midheight of the mock missile's cylindrical section is at $z_c = 0.594$ m. The dipole array is at a height of $z_c = 0.594$ m and is illuminating the missile at the middle of the cylindrical section. As figure 13 shows, the voltage across the impedance load is 6.2 V when the dipole array distance from the mock missile is $\rho_c = b + \lambda/2$ or ≈ 1.5 m. The voltage across the impedance load is 1.7 V when the dipole array distance from the mock missile is $\rho_c = b + 2\lambda$ or ≈ 6 m. This is a change of 11.2 dB due to moving the dipole array position away from the missile axis. NOTE: The array is on the x-z plane and is pointed toward the y-axis direction. The array is displaced along a line parallel to the z-axis. The expected change due to moving away in range ($1/R^2$ distance factor) is 12.04 dB. This is less than 1 dB larger than the change observed in the voltage across the impedance load. Referring back to condition 1, the mock missile is in the far field of the array source for both positions of the source ($\rho_c = b + \lambda/2$ and $\rho_c = b + 2\lambda$).

Condition 6 Excitation Source: 4 by 4 dipole array (sheet of current or z-x plane represented by 4 by 4 unity strength z-directed dipole array). The 4 by 4 dipole array is centered at $(x_c, 0, z_c)$ and located on the x-z axis. As figure 14 shows, the dipole array is displaced along a line in the x-z plane and its height is constant (z_c is fixed). Plots of the voltage across the impedance load versus the array source's distance from the mock missile (ρ_c is varied from ≈ 0.6 to 6 m) are shown in figure 15.

Condition 6 Analysis: as figure 14 shows, the excitation source is a 4 by 4 dipole array (sheet of current on the x-z plane represented by a 4 by 4 unity strength z-directed dipole array). At height $z_c = 1.187$ m, the tapered cone on top of the cylindrical section is attached. The dipole array is at a height of $z_c = 1.187$ m and is illuminating the missile at the point where the taper begins, on top of the cylindrical section. Figure 15 shows the voltage across the impedance load is 9 V when the dipole array distance from the mock missile is $\rho_c = 0.75$ m. The voltage across the impedance load is 1.5 V when the dipole array distance from the mock missile is 6 m. This is a change of 15.56 dB due to moving the dipole array position further away from the missile axis ($\rho_c = 0.75$ m to $\rho_c = 6$ m). The expected change due to moving away in range ($1/R^2$ distance factor) is 18.06 dB. This is 2.5 dB higher than the change observed in the voltage across the impedance load. NOTE: The dipole array is displaced along a line in the x-z plane and is pointed toward the y-axis direction.

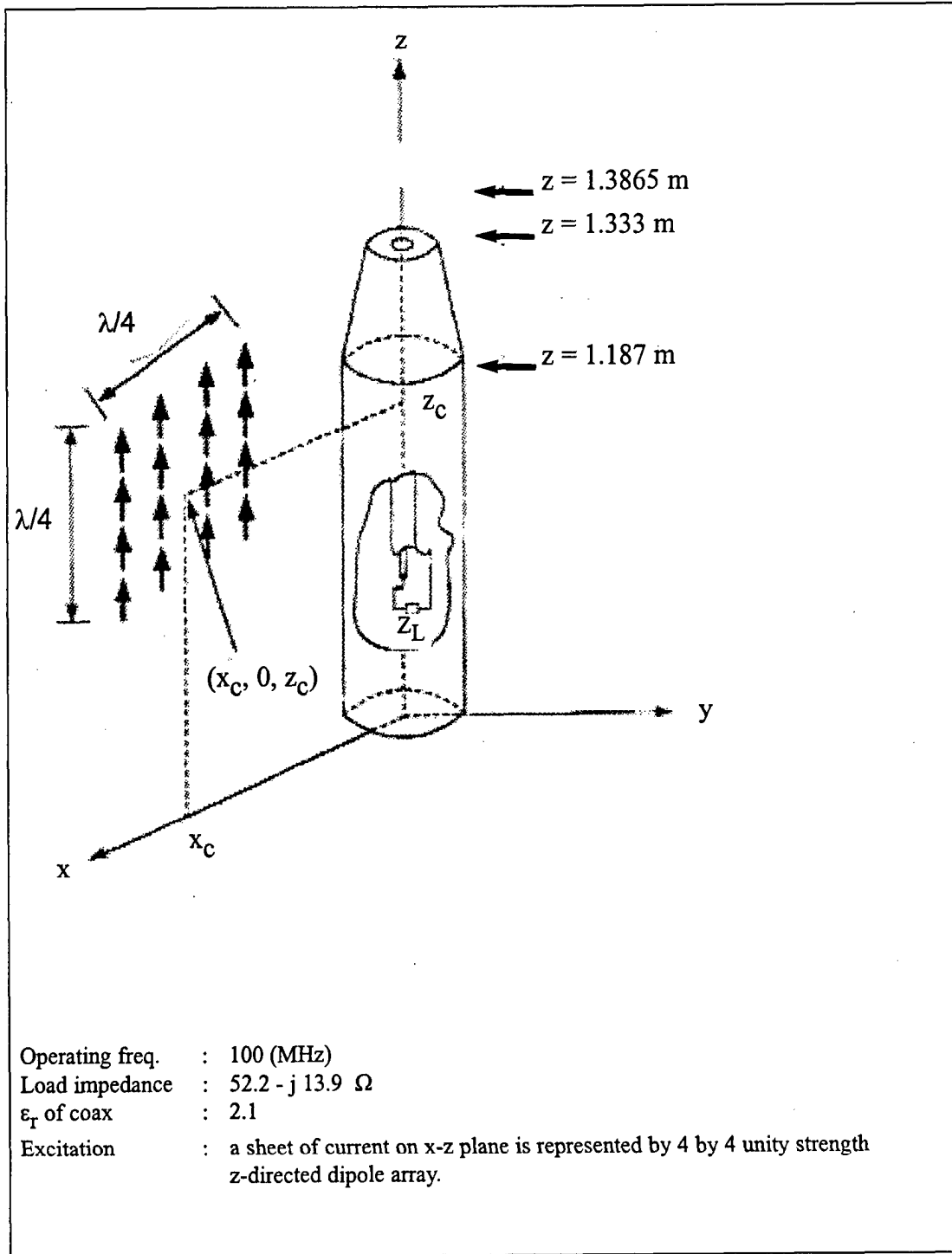


Figure 14. Geometry: 4 by 4 dipole array centered at $(x_c, 0, z_c)$ and located on the x-z plane. It is displaced along a line in the x-z plane and its z position is constant.

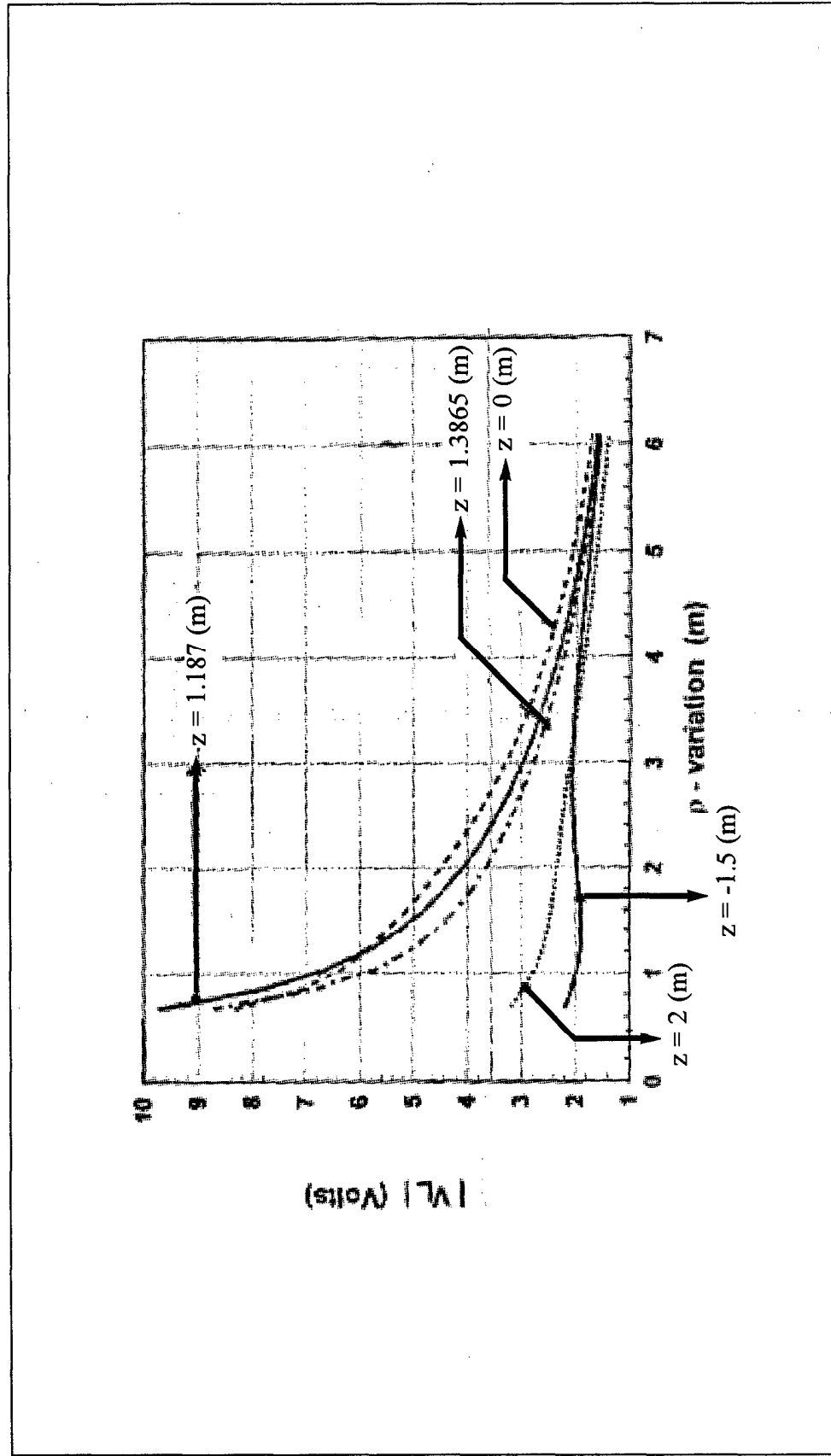


Figure 15. Voltage plots: Sheet current represented as 4 by 4 dipole array varied along ρ direction with a fixed z location.

Condition 7 Excitation Source: 4 by 4 dipole array (sheet of current parallel to y-z plane represented by 4 by 4 unity strength z-directed dipole array). The 4 by 4 dipole array is centered at $(x_c, 0, z_c)$ and is parallel to the y-z plane. As figure 16 shows, the dipole array is displaced along a line parallel to the x-axis and the array's height is constant (z_c is fixed). Plots of the voltage across the impedance load versus array height along the line parallel to the x-axis is shown in figure 17. The array distance from the mock missile was varied from $x_c = b + \lambda/5$ to $x_c = b + 2\lambda$.

Condition 7 Analysis: As figure 16 shows, the excitation source is a 4 by 4 dipole array (sheet of current parallel to the y-z plane represented by 4 by 4 unity strength z-directed dipole array). The array is displaced along a line parallel to the x-axis and is pointed toward the (negative) x-axis direction. The midheight of the mock missile's cylindrical section is at $z_c = 0.594$ m. The dipole array is at a height of $z_c = 0.594$ m and is illuminating the middle of the missile's cylindrical section. As figure 17 shows, the voltage across the impedance load is 5.9 V when the dipole array distance from the mock missile is $x_c = b + \lambda/2$ or ≈ 1.5 m. The voltage across the impedance load is 1.6 V when the dipole array distance from the mock missile is $x_c = b + 2\lambda$ or ≈ 6 m. This is a change of 11.32 dB due to moving the dipole array position further away from the missile axis. The expected change due to moving away in range ($1/R^2$ distance factor) is 12.04 dB. This is just slightly (0.72 dB) larger than the change observed in the voltage across the impedance load.

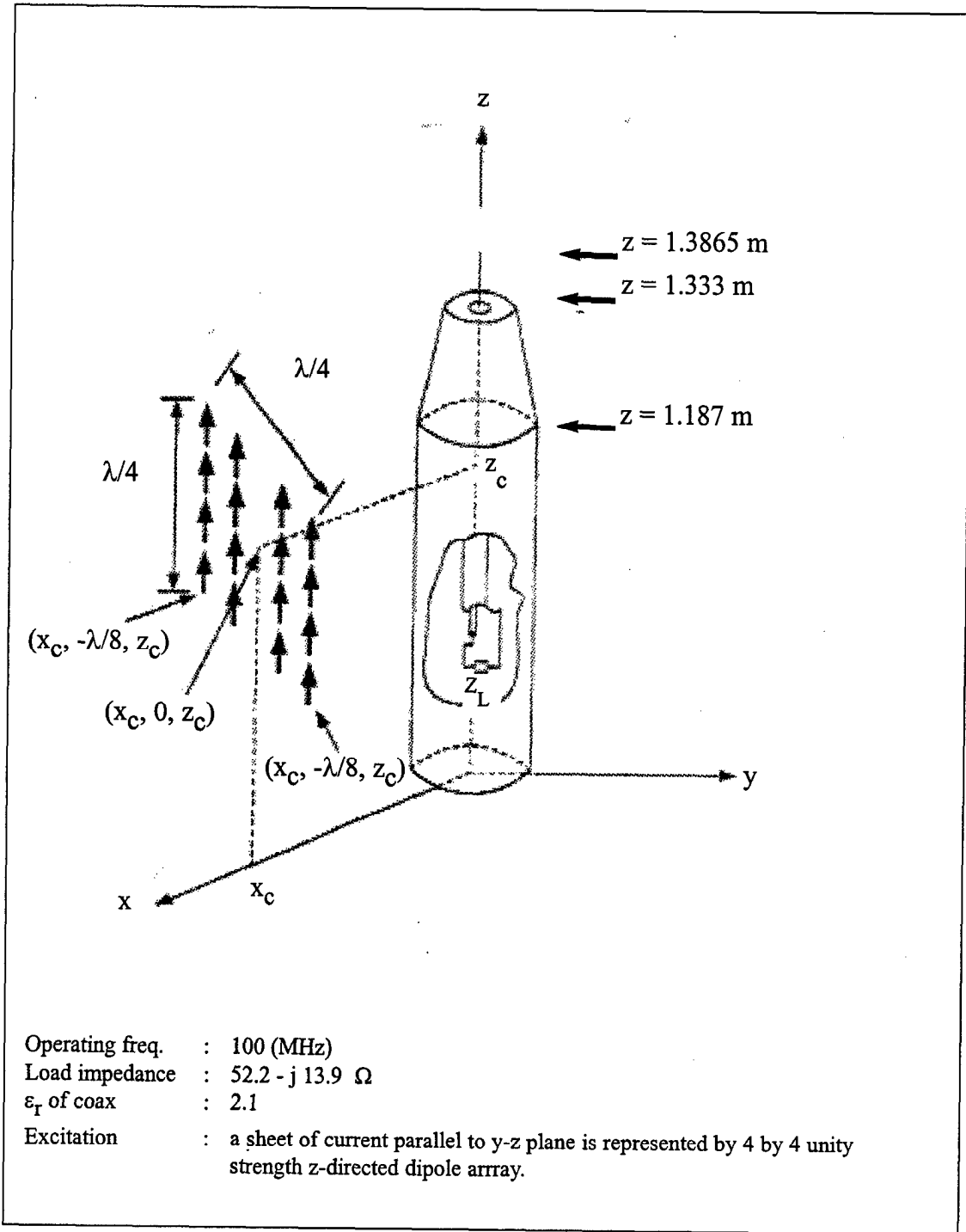


Figure 16. Geometry: 4 by 4 dipole array centered at $(x_c, 0, z_c)$ and is parallel to y-z plane. It is displaced along a line parallel to the x-axis and z_c is constant.

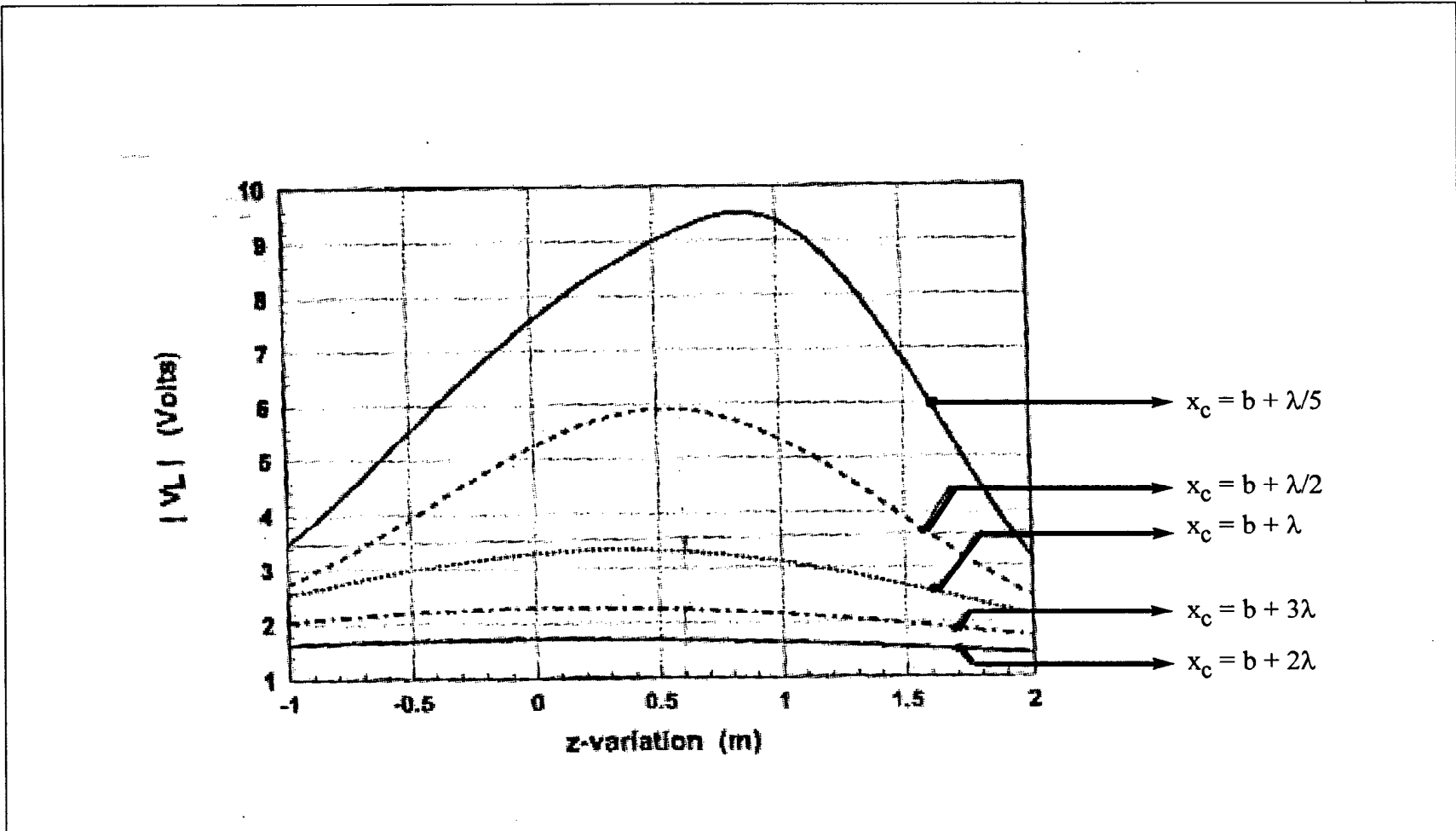


Figure 17. Voltage plots: Sheet current represented as 4 by 4 dipole array parallel to y - z plane, displaced along z direction.

Condition 8 Excitation Source: 4 by 4 dipole array (sheet of current parallel to the y-z plane represented by 4 by 4 unity strength z-directed dipole array). The dipole array is centered at $(x_c, 0, z_c)$ and is parallel to the y-z plane. As figure 18 shows, the dipole array is displaced along a line parallel to the z-axis and the array's distance from the z-axis is constant (x_c is fixed). Plots of the voltage across the impedance load versus the array's distance from the mock missile's axis (ρ_c is varied from ≈ 0.6 to 6 m) are shown in figure 19.

Condition 8 Analysis: as figure 18 shows, the excitation source is a 4 by 4 dipole array (sheet of current parallel to the y-z plane represented by 4 by 4 unity strength z-directed dipole array). The array is displaced along a line parallel to the z-axis and the beam formed is pointed toward the (negative) x-axis direction. At height $z_c = 1.187$ m, the tapered cone on top of the cylindrical section is attached. The dipole array is at a height of $z_c = 1.187$ m and is illuminating the missile at the point where the taper begins, on top of the cylindrical section. As figure 19 shows, the voltage across the impedance load is 8.1 V when the dipole array distance from the mock missile is $\rho_c = 0.7$ m. The voltage across the impedance load is 1.6 V when the dipole array distance from the mock missile is 6 m. This is a change of 14.08 dB due to moving the dipole array position further away from the missile axis ($\rho_c = 0.7$ m to $\rho_c = 6$ m). The expected change due to moving away in range ($1/R^2$ distance factor) is 18.6 dB. This is 4.5 dB larger than the change observed in the voltage across the impedance load.

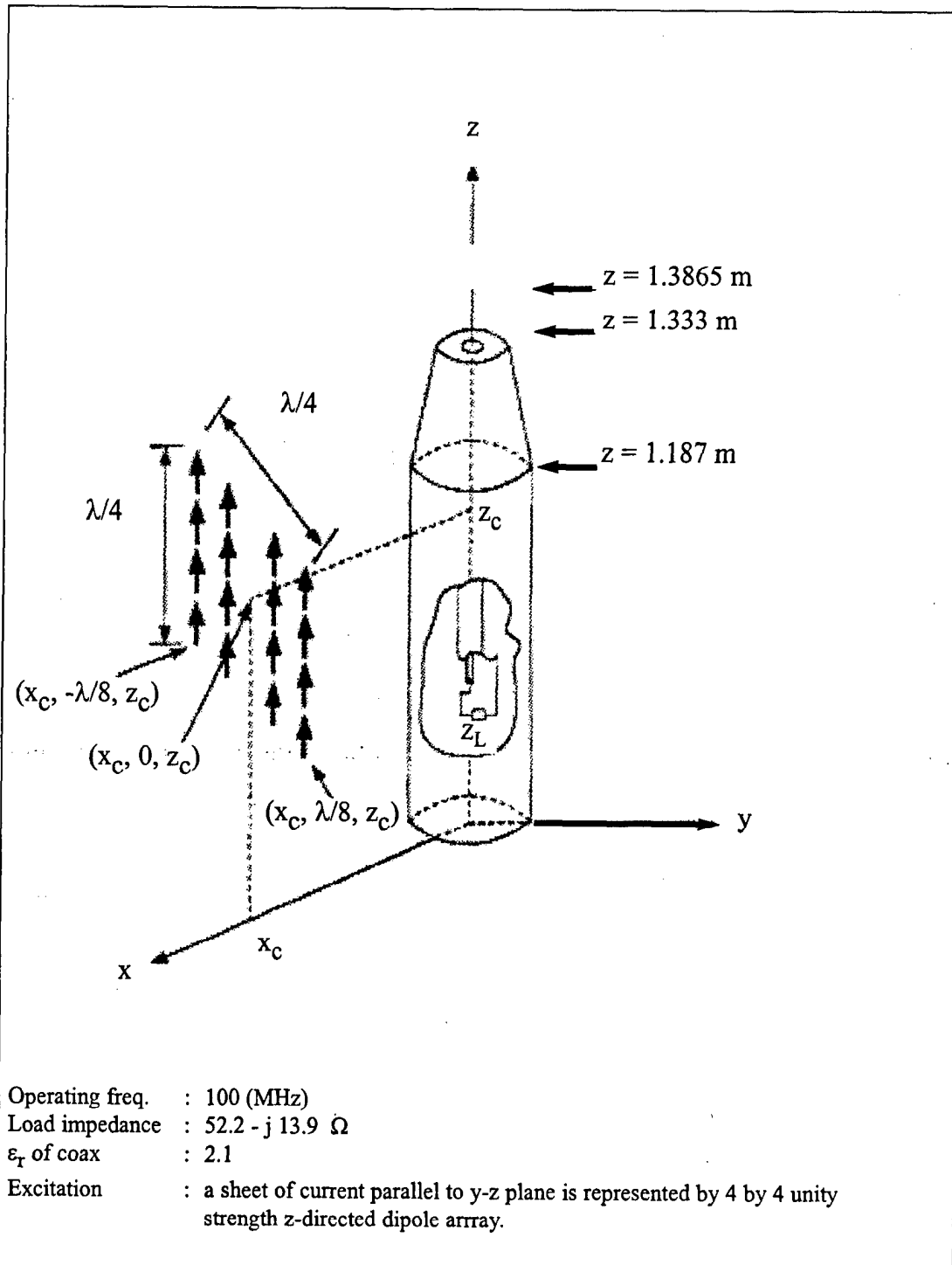


Figure 18. Geometry: 4 by 4 dipole array centered at $(x_c, 0, z_c)$ and is parallel to y-z plane. It is displaced along a line parallel to the z-axis and x_c is constant.

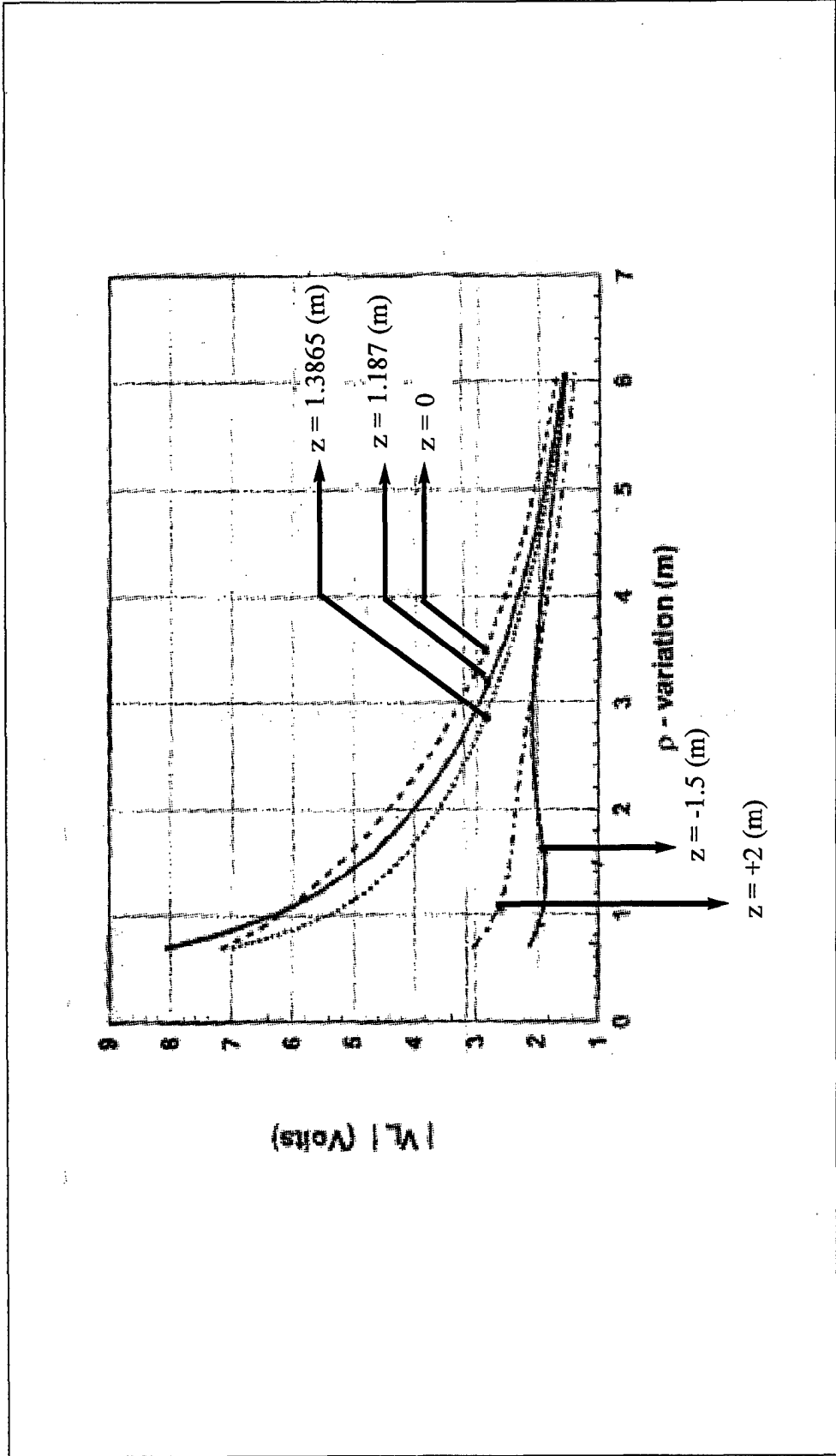


Figure 19. Voltage plots: Sheet current represented as 4 by 4 dipole array parallel to y-z plane, displaced along ρ direction with fixed z .

4. Conclusions

The first investigation by Tsai showed that as much as a *factor of two (2)* difference can exist in the skin currents induced by the source operating at near field versus when the source is at far field. [1] This occurred for broadside incidence and at 100 MHz. In this case, the skin current was smaller at near field than at far field. The *factor of two (2)* difference in the skin current equates to a *6 dB increase* in power requirements when the source is operating at the near field zone. Phase curvature of the incident wave plays a significant role in determining what occurs at near field.

Applying this to the E³ test methodology operating at near field, skin currents induced by the source can have as much as a factor of two error or difference than when the source is at far field because of the phase curvature of the incident wave. The model used in this investigation was the thin wire or rod and was simplistic. Direct application of results obtained by this investigation cannot realistically be applied to the E³ situation where the target is very complex. But the trend brought about by the near field versus far field results can be applied. Because the incident field in this investigation was held constant, the effects of the $1/R^2$ distance factor has been taken into account.

The difference in skin currents induced by the source is due mainly to the near field geometry as previously discussed.

The second investigation by Professor Butler is not as easily deduced for application to the E³ test methodology operating at near field. [2] Numerically solving the integral equations for the voltage across the impedance load inside the mock missile made no provisions to keep the incident field constant while moving from near field to far field. For this reason, the $1/R^2$ distance factor overshadows the changes incurred in the voltage across the impedance load due to moving the excitation source from near field to far field. In all eight conditions involving different excitation sources and source geometries, the expected change due to moving away in range ($1/R^2$ distance factor) is greater than the change in the calculated voltage across impedance load due to moving the excitation source further away from the missile axis.

Conditions 7 and 8, compared to the other conditions, best emulate the test conditions present at the E³ tests. The dipole array at far field exhibits a beam radiation. As the dipole array is brought closer to the missile, simulating near

field conditions, the beam is no longer definable and the circular impinging wave is very complex.

Of course, the radiation exhibited by horns, which are extensively used for the higher frequencies and the log-periodic antennas used for the lower frequencies, are different than the radiation beam exhibited by the dipole array. The radiation pattern is a far field concept and has little meaning insofar as near fields are concerned. However, at a distance of $\lambda/2$ from a dipole, the radiation field dominates over the static and induction fields.

Of significant importance in this second investigation is the fact that the calculated voltage across the impedance load is *inside* the mock missile. At low frequencies, i.e., 100 MHz, the body resonances play an important role and the near field effects are dominated by the $1/R$ factor. Voltage across the impedance load is maximum when the missile is illuminated at midpoint. Moving the illumination point on either side, just off midpoint, quickly reduces the voltage developed across the impedance load. At higher frequencies (greater than 600 MHz), the body or physical apertures of a test object play significantly in the coupling phenomena. The near field effects due to the sphericity of the impinging wave becomes more prominent. The target used in the E^3 test are more complex than the mock missile or the thin rod. To stress the target under test for EM survivability, the target should be illuminated by the excitation source operating at near field directly at the suspect apertures to attain good coupling.

When compared to far field testing, it appears that near field testing can be in error due to near-field complexities by as much as 6 dB and possibly more for more complex sources and test objects. Whether this error is considered significant is a matter to be considered by the E^3 community. Near field effects are always lower than far field effects at the same field strength as seen in both investigations.

5. Additional Discussions

There appear to be some controversies concerning what is considered near field and what is far field when performing E^3 tests, such as the EMV.

There are two far field criteria that must be met when performing valid EMV tests, Hazards of EM Radiation to Ordnance (HERO) tests, Special EM Interference (SEMI) tests and radar cross section measurements.

First Criterion. The test object must be far enough from the transmitting antenna that the incident power density at the point where the center of the antenna beam intersects the test object can be calculated from the following equation:

$$P_d = P_o G/4 \pi R^2 \quad (1)$$

where

- P_d = the incident power density at the intersection point,
- R = the distance from the transmitting antenna to the intersection point,
- P_o = the power into the antenna
- G = the antenna gain.

The criterion for this equation to be valid is:

$$R > 2 d^2/\lambda \quad (2)$$

where

- λ = the wavelength of the electromagnetic radiation
- d = the largest dimension of the transmitting antenna (e.g., the diameter of a circular dish or the largest dimension of a rectangular horn).

This is the far field criterion typically used by radar engineers to ensure that field strength calculations are valid.

Second Criterion. The test object must be far enough from the transmitting antenna that the test object is uniformly illuminated by the incident field. When conducting EMV or SEMI investigations or making radar cross section measurements, the objective is to determine the response of the test object to a plane wave EM field. Since plane wavefronts are obtainable only at infinite distances, some limits must be specified. A commonly specified criterion for valid testing is that with the longest dimension d of the test object placed perpendicular to the center of the transmitting antenna beam, the phase difference between the center and edge of the test object shall be no greater than $\lambda/16$. Under these conditions, the test object is essentially uniformly illuminated and plane wave conditions are attained to the extent necessary for valid results. The phase and amplitude of the EM field are uniform over the test object. This criterion has been adopted by the test community, based on theoretical calculations and cumulative test experience.

Figure 20 shows the geometry for determining uniform EM field illuminations. For the test object to be at far field conditions, the phase difference between the center and edge of the test object shall be no greater than $\lambda/16$. In other words, for essentially uniform illumination, L (the distance from the transmitting antenna to the edge of the test object) must not be greater than $R + \lambda/16$.

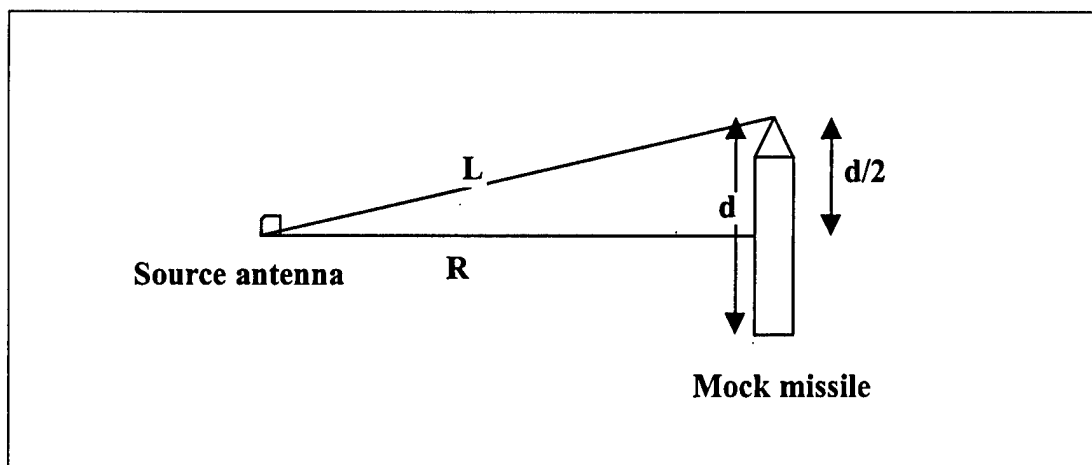


Figure 20. Geometry for determining uniform EM field illumination.

$$L \leq R + \lambda/16$$

$$L^2 = R^2 + d^2/4$$

$$R^2 + 2\lambda R/16 + \lambda^2/256 \geq R^2 + d^2/4$$

$$R \geq 2 d^2/\lambda - \lambda/32$$

$\lambda/32$ is very small and is negligible

Conditions for far field:

$$R \geq 2 d^2/\lambda$$

NOTE: d is the largest dimension of the test object.

For valid radar cross section measurements, EMV, SEMI and HERO testing, both of the aforementioned criteria must be met. Therefore, in the equation

$$R \geq 2 d^2 / \lambda \quad (3)$$

d is the largest dimension of the transmitting antenna, or the test object, *whichever is larger*.

When conducting E³ investigations, such as EMV and HERO tests, the test object is often “spot” illuminated instead of totally illuminated by the transmitting source antenna. The test object is not uniformly illuminated. It is not feasible or practical to satisfy the criteria because of the power limitations of available sources and because of safety reasons. However, when compromising this criteria for practical reasons, it must be recognized that body resonances that would be excited in a plane wave field may be absent or only weakly present when the field is not uniform over the test object. In addition, the combined effects from field penetration through two or more apertures simultaneously may not be discovered.

Based on the results of this Survivability/Lethality Analysis Directorate report, everyone involved in the E³ investigations should be aware that anomalies, uncertainties, or errors do exist in measurements made at the Fresnel zone or near field. Near field testing when compared to far field testing can be in error due to near field complexities by as much as 6 dB and possibly more for more complex sources and test objects.

References

1. Tsai, L., T. K. Wu, R. D. Darone, and G. L. Brown, *Some Aspect of Valid EMC Testing of Missiles*, U.S. Missile Command, Redstone Arsenal, AL, IEEE Transactions of Electromagnetic Compatibility, Vol. EMC-20, No. 2, May 1978.
2. Butler, C. and K. Yegin, *Complex Near Source Coupling To Probe on Mock Missile*, Clemson University, July 1998.
3. Schelkunoff, S. A., *Field Equivalence Theorems, Commun.*, Pure Appl. Math., Vol 4, pp. 43-59, June 1951.

Acronyms and Abbreviations

dB	decibels
E ³	electromagnetic environmental effects
EM	electromagnetic
EME	electromagnetic environment
EMV	electromagnetic vulnerability
HERO	Hazards of EM Radiation to Ordnance
SEMI	Special Electromagnetic Interference

Distribution

	Copies
DEFENSE TECH INFO CTR ATTN DTIC OCA J CHIRAS 8725 JOHN J KINGMAN RD STE 0944 FT BELVOIR VA 22060-6218	2
OUSD AT S&T AIR WARFARE ATTN DR RAINIS RM 3E139 3090 DEFENSE PENTAGON WASHINGTON DC 20310-3090	1
OUSD AT S&T LAND WARFARE ATTN MR VILU RM 3B1060 3090 DEFENSE PENTAGON WASHINGTON DC 20310-3090	1
OASD C31 ATTN DR SOOS RM 3E194 6000 DEFENSE PENTAGON WASHINGTON DC 20301-6000	1
UNDER SEC OF THE ARMY DUSA OR RM 2E660 102 ARMY PENTAGON WASHINGTON DC 20310-0102	1
ASST SECY ARMY RESEARCH DEVELOPMENT ACQUISITION SARD ZD RM 2E673 103 ARMY PENTAGON WASHINGTON DC 20310-0103	1
ASST SECY ARMY RESEARCH DEVELOPMENT ACQUISITION SARD ZP RM 2E661 103 ARMY PENTAGON WASHINGTON DC 20310-0103	1
ASST SECY ARMY RESEARCH DEVELOPMENT ACQUISITION SARD ZS RM 3E448 103 ARMY PENTAGON WASHINGTON DC 20310-0103	1

OADCSOPS FORCE DEV DIR ATTN DAMO FDW RM 3C630 460 ARMY PENTAGON WASHINGTON DC 20310-0460	1
OADCSOPS FORCE DEV DIR ATTN DAMO FDT MR DENNIS SCHMIDT 460 ARMY PENTAGON WASHINGTON DC 20310-0460	1
US MILITARY ACADEMY MATH SCI CTR EXCELLENCE ATTN MADN MATH LTC ENGEN THAYER HALL WEST POINT NY 10996-1786	1
HQ USAMC DEP CHF OF STAFF FOR RDA ATTN AMCRDA 5001 EISENHOWER AVE ALEXANDRIA VA 22333-0001	1
HQ USAMC PRINCIPAL DEP FOR ACQSTN ATTN AMCDCG A 5001 EISENHOWER AVE ALEXANDRIA VA 22333-0001	1
HQ USAMC PRINCIPAL DEP FOR TECH ATTN AMCDCG T 5001 EISENHOWER AVE ALEXANDRIA VA 22333-0001	1
ARMY TEST EVAL COM AMSTE TM S APG MD 21005-5055	1
US ARMY EVAL ANALYSIS CTR ATTN CSTE EAC MR HUGHES 4120 SUSQUEHANNA AVE APG MD 21005-3013	1
US ARMY EVAL ANALYSIS CTR ATTN CSTE EAC SV DR HASKELL 4120 SUSQUEHANNA AVE APG MD 21005-3013	1

ARMY TRNG & DOCTRINE COM 1
ATTN ATCD B
FT MONROE VA 23561-5000

ARMY TRADOC ANL CTR 1
ATTN ATRC W
MR KEINTZ
WSMR NM 88002-5502

ARMY RESEARCH LABORATORY 1
ATTN AMSRL DD
J ROCCHIO
2800 POWDER MILL RD
ADELPHI MD 20783-1197

ARMY RESEARCH LABORATORY 1
ATTN AMSRL D
R WHALIN
2800 POWDER MILL RD
ADELPHI MD 20783-1197

ARMY RESEARCH LABORATORY 1
ATTN AMSRL SL
DR WADE
APG MD 21005-5068

ARMY RESEARCH LABORATORY 1
ATTN AMSRL SL
PLANS AND PGMS MGR
WSMR NM 88002-5513

ARMY RESEARCH LABORATORY 1
ATTN AMSRL SL E
DR STARKS
APG MD 21010-5423

ARMY RESEARCH LABORATORY 1
ATTN AMSRL SL B
MS SMITH
APG MD 21005-5068

ARMY RESEARCH LABORATORY 1
ATTN AMSRL SL
MR BEILFUSS
APG MD 21005-5068

ARMY RESEARCH LABORATORY 1
ATTN AMSRL SL E
MR SHELBURNE
WSMR NM 88002-5513

ARMY RESEARCH LABORATORY 1
ATTN AMSRL CS AL TA
2800 POWDER MILL RD
ADELPHI MD 20783-1145

ARMY RESEARCH LABORATORY ATTN AMSRL CS AL TP 2800 POWDER MILL RD ADELPHI MD 20783-1145	1
ARMY RESEARCH LABORATORY ATTN AMSRL CI LL 2800 POWDER MILL RD ADELPHI MD 20783-1145	3
ARMY RESEARCH LABORATORY ATTN AMSRL CI LP BLDG 305 ABERDEEN MD 21005-5068	2
ARMY RESEARCH LABORATORY ATTN JOY ARTHUR AMSRL SL EV WSMR NM 88002-5513	2
Record copy	1
TOTAL	38